DNA-Based Methodologies for the Authentication of *Eleutherococcus senticosus* and *Rhodiola rosea*

Arthur Baldomero Taques

Dissertation submitted to Escola Superior Agrária de Bragança to obtain the Degree of Master in Biotechnological Engineering under the scope of the double diploma with Universidade Tecnológica Federal do Paraná – Campus Ponta Grossa

Supervisors

Professor Joana S. Amaral

Professor Juliana Vitoria Messias Bittencourt

Professor Maria Alice Pinto

Bragança 2025

This work was supported by the FCT (Fundação para a Ciência e Tecnologia) through the project "POIROT: novel methods and approaches for detecting the illegal addition of Pharmaceutical drugs and botanical adulteration in plant food supplements" (DOI:10.54499/PTDC/SAU-PUB/3803/2021).

ACKNOWLEDGEMENTS

I would like to thank everyone who has been with me throughout this journey of my life, and all those who helped me, advised me, and supported me.

I am deeply grateful to Professor Joana, Mônica, and Joana (Juca), as without your guidance, patience and teachings, it would not have been possible to complete this stage.

To my friends Chaimaa, Saliha, Meriem, Mariem, Khadija, Eduardo, and Manu, who brought me countless moments of joy and became a family to me, my heartfelt thank you!

ABSTRACT

Eleutherococcus senticosus, commonly known as Siberian ginseng, is an adaptogenic plant widely used in traditional Chinese and Russian medicine, recognized for its effects on physical endurance, cognitive performance, and immune modulation. Its growing use in the herbal, nutraceutical, and pharmaceutical industries has increased the demand for reliable methods to ensure the authenticity of commercial products. Similarly, *Rhodiola rosea*, a high-value medicinal species native to mountainous regions of Europe and Asia, is frequently used to reduce fatigue and enhance mental performance. Both species face significant risks of adulteration and substitution, especially when marketed in processed forms that hinder morphological identification. Therefore, this study aimed to develop molecular tools for the authentication of *E. senticosus* and *R. ro*sea in commercial herbal products.

Species- and genus-specific primers targeting barcode regions were designed and evaluated, including genus-specific primers coupled with real-time PCR and high-resolution melting (HRM) analysis. For R. rosea, the tested approaches were unable to reliably discriminate the species, as samples originating from botanical gardens clustered separately. Further investigation is required to determine whether these results reflect intraspecific genetic variation or sample misidentification.

For *E. senticosus*, the primers designed for the species-specific amplification revealed to amplify also other *Eleutherococus* species. However, the primers proved to be specific for *Eleutherococcus* genus, without presenting cross-reactivity with other medicinal plants used for similar therapeutic purposes, and were therefore evaluated by real-time PCR coupled with HRM analysis. The primer set EleuFDS-F/EleuFDS-R, targeting the farnesyl diphosphate synthase gene, provided the highest discriminatory power, allowing the differentiation of *E. sent*icosus from *E. leucorrhizus*, *E. lasiogyne*, *E. henryi*, and *E. divaricatus*. Subsequent application of the developed methodology to 12 commercial samples, including herbal products and food supplements labeled as being Siberian ginseng, was only able to authenticate two samples.

Overall, this study aimed to provide accurate and accessible techniques to improve quality control, traceability, and safety in the use of medicinal plant species, suggesting a high level of adulteration among Siberian ginseng products.

Keywords: Siberian Ginseng, golden root, medicinal plant adulteration, real-time PCR, HRM.

RESUMO

Eleutherococcus senticosus, conhecido como ginseng-siberiano, é uma planta adaptogénica amplamente utilizada na medicina tradicional chinesa e russa, reconhecida por seus efeitos sobre a resistência física, função cognitiva e modulação do sistema imunitário. Sua crescente aplicação nas indústrias de fitoterápicos, suplementos alimentares e produtos farmacêuticos tem intensificado a necessidade de métodos confiáveis para garantir a autenticidade dos produtos comerciais. De forma semelhante, *Rhodiola rosea*, também de grande valor medicinal, é uma espécie adaptogénica nativa de regiões montanhosas da Europa e Ásia, frequentemente utilizada para combater a fadiga e melhorar o desempenho mental. Ambas as espécies enfrentam riscos significativos de adulteração e substituição, especialmente quando comercializadas em formas processadas que dificultam a identificação morfológica.

Este trabalho tem como objetivo desenvolver ferramentas baseadas em biologia molecular para a autenticação de *Eleutherococcus senticosus* e *Rhodiola rosea*, em produtos à base de plantas medicinais e suplementos alimentares.

Foram desenhados e avaliados primers específicos de espécie e de género direcionados para regiões barcode, incluindo primers específicos de género acoplados à PCR em tempo real com análise de melting de alta resolução (HRM). No caso de *R. rosea*, as abordagens testadas não permitiram discriminar a espécie de forma fiável, uma vez que amostras provenientes de jardins botânicos se agruparam em clusters distintos. São necessários estudos adicionais para determinar se estes resultados se devem a variação genética intraespecífica ou a uma possível identificação incorreta das amostras.

Relativamente a *E. senticosus*, os primers desenhados para amplificação específica da espécie revelaram também amplificar outras espécies de *Eleutherococcus*. No entanto, os primers demonstraram ser específicos para o género *Eleutherococcus*, não apresentando reatividade cruzada com outras plantas medicinais utilizadas para fins terapêuticos semelhantes, tendo sido, por isso, avaliados por PCR em tempo real acoplada à análise HRM. O conjunto de primers EleuFDS-F/EleuFDS-R, com alvono gene da farnesil difosfato sintase, apresentou o maior poder discriminatório, permitindo a diferenciação de *E. senticosus* de *E. leucorrhizus*, *E. lasiogyne*, *E. henryi* e *E. divaricatus*. A aplicação subsequente da metodologia desenvolvida a 12 amostras comerciais, incluindo produtos à base de plantas e suplementos alimentares rotulados como ginseng-siberiano, permitiu autenticar apenas duas amostras.

De forma geral, este estudo teve como objetivo disponibilizar técnicas precisas e

acessíveis para melhorar o controlo de qualidade, a rastreabilidade e a segurança na utilização de espécies de plantas medicinais, sugerindo um elevado nível de adulteração entre os produtos comerciais de ginseng-siberiano.

Palavras chaves: ginseng Siberiano, raiz dourada, adulteração de plantas medicinais, PCR em tempo real, HRM.

LIST OF ABBREVIATIONS

ARMS — Amplification Refractory Mutation System

Bar-HRM — Barcode High-Resolution Melting

bp — base pair(s)

CBOL — Consortium for the Barcode of Life

CE — Capillary Electrophoresis

COI — Cytochrome c oxidase subunit I

DAD — Diode-Array Detector

DNA — Deoxyribonucleic Acid

EG — Eukaryotic global primers targeting 18S rRNA mini-barcode (universal plant marker)

EMA — European Medicines Agency

EU — European Union

GC — Gas Chromatography

GC content — Guanine–Cytosine content (percent GC in DNA)

HCA — Hierarchical Cluster Analysis

H-NMR (^{1}H NMR) — Proton Nuclear Magnetic Resonance

HPLC — High-Performance Liquid Chromatography

HPTLC — High-Performance Thin-Layer Chromatography

HR-MS — High-Resolution Mass Spectrometry

HRM — High-Resolution Melting

ITS / ITS2 — Internal Transcribed Spacer / Internal Transcribed Spacer 2

LC-MS — Liquid Chromatography–Mass Spectrometry

matK — maturase K (plastid gene)

MS — Mass Spectrometry

NGS — Next-Generation Sequencing

NTC — No-Template Control

PCA — Principal Component Analysis

PCR — Polymerase Chain Reaction

PFS — Plant Food Supplements

qPCR — quantitative PCR (real-time PCR)

rbcL — ribulose-1,5-bisphosphate carboxylase/oxygenase large subunit gene

RFLP — Restriction Fragment Length Polymorphism

SCAR — Sequence Characterized Amplified Region

SNP — Single Nucleotide Polymorphism

SSR — Simple Sequence Repeat

THMP(s) — Traditional Herbal Medicinal Product(s)

TLC — Thin-Layer Chromatography

Tm — Melting temperature (DNA)

UHPLC / UPLC — (Ultra-)High-Performance Liquid Chromatography

WHO — World Health Organization

LIST OF FIGURES

LIST OF TABLES

Summary

1. OBJECTIVES

The utilization of medicinal plants represents one of the oldest therapeutic strategies employed by humankind and continues to play an important role in the search for novel bioactive compounds. Their phytochemical complexity has provided relevant pharmacological agents with antioxidant, immunomodulatory, and adaptogenic properties, among others. In recent decades, the increasing demand for natural products and the expansion of the nutraceutical and phytopharmaceutical markets have highlighted the necessity of reliable approaches to guarantee authenticity, quality, and consumer safety.

Within this context, *Eleutherococcus senticosus* and *Rhodiola rosea* are two of the most widely recognized adaptogenic species. *E. senticosus*, commonly referred to as Siberian ginseng, is distributed throughout northeastern Asia and has been extensively used in traditional Russian and Chinese medicine. Its pharmacological properties are attributed mainly to eleutherosides, which have been associated with improved physical performance, immune system modulation, and cognitive resilience. These characteristics justify its wide incorporation into food supplements and functional formulations. *R. rosea*, also known as golden root, occurs naturally in cold and high-altitude regions of Europe and Asia. Traditionally employed to counteract fatigue and enhance mental performance, it is particularly valued for its salidroside and rosavin derivatives, which are considered chemical markers of the species. The growing demand for *R. rosea* in the European and global markets has consolidated its status as a high-value medicinal plant, while simultaneously increasing the risks of substitution and adulteration with morphologically or chemically similar taxa.

Both *E. senticosus and R. rosea* are often marketed in processed forms, such as fragmented plants, powders, extracts, or encapsulated preparations, which preclude morphological identification and complicate taxonomic verification. Furthermore, the existence of closely related species (*Rhodiola crenulata*, *Rhodiola kirilowii*, or other *Eleutherococcus* spp.) and the indiscriminate use of the common "ginseng" designation facilitate both accidental misidentification and deliberate adulteration. These practices compromise product integrity and reinforce the need for molecular authentication tools with high sensitivity and specificity.

The present study aims to develop molecular methodologies for the authentication of *E. senticosus* and *R. rosea*, which can be applied to commercial samples to discriminate between

the species and their most common adulterants. To this end, species-specific primers targeting polymorphic genomic regions will be designed and tested. Their performance will be assessed through conventional PCR and real-time PCR, to evaluate specificity and sensitivity. High-Resolution Melting (HRM) analysis will be further applied to discriminate species based on melting curve profiles. Finally, the methodologies will be tested in commercial supplements to evaluate their applicability under real-market conditions, contributing to enhanced traceability, safety, and regulatory compliance in the use of medicinal plant products.

2. INTRODUCTION

2.1 Medicinal plants

Throughout history, humanity has relied on plants not only to meet dietary needs but also to treat a wide variety of diseases. Natural products have played a fundamental role in the historical development of modern medicine and remain essential in the ongoing search for new therapeutic agents. Several important discoveries have emerged from natural sources, including compounds with anticancer, anti-inflammatory, and analgesic activity (Sen et al., 2015).

In this context, medicinal plants represent a unique and renewable source for the discovery of therapeutically active biomolecules, given their vast structural and biological diversity. However, only a limited fraction of the plant kingdom has been explored for this purpose. While chemical diversity continues to provide innovative opportunities for the development of new treatments, genomic research contributes to the identification of molecular targets that enable specific screening assays (Bezerra et al., 2013). Thus, the exploration of the therapeutic potential of plants should not be seen merely as an alternative, but rather as a valuable complement to conventional medicine, especially in a context of increasing demand for natural and sustainable approaches (Chiang et al., 2015).

Pharmaceutical industries make use of both plant extracts and synthetic derivatives, with natural structures often serving as the basis for chemical modifications that generate medicines with adequate pharmacological activity and low toxicity. Despite the wide use of synthetic drugs, it is estimated that approximately 80% of the world's population relies on treatments with herbal medicines or plant extracts (WHO, 2012; Bezerra et al., 2013). In recent years, there has also been a sharp increase in the consumption of plant-based food supplements. Several factors contribute to this trend: the growing public interest in healthier lifestyles, the perception that these products support disease prevention and well-being, dissatisfaction with the adverse effects of synthetic drugs, rising healthcare costs, and the widespread belief that natural products are inherently safer (El-Ahmady et al., 2016; Sasikumar et al., 2016; WHO, 2013).

In the European Union (EU), medicinal plants are subject to specific regulation to ensure the quality, safety, and efficacy of products. Directive 2004/24/EC (the Herbal Directive) complements Directive 2001/83/EC by establishing harmonized criteria for the authorization, commercialization, and use of traditional herbal medicinal products (THMPs), thus standardizing procedures across Member States (EMA, 2024). To be marketed in Europe, products must

comply with procedures overseen by national competent authorities, the most accessible being the “Traditional Use Registration.” This pathway applies to products with at least 30 years of documented use, including 15 years within the EU, and intended for use without medical supervision. In such cases, clinical trials are not required, provided there is sufficient evidence of safety and plausible efficacy (EMA, 2024; Calapai et al., 2018). This regulatory framework contributes both to public health protection and to consistency within the European sector.

In this context, adaptogenic plants such as *Rhodiola rosea* and *Eleutherococcus senticosus* have received particular scientific and commercial attention. *R. rosea*, traditionally used to combat fatigue and improve cognitive performance, contains bioactive compounds such as rosavins and salidroside, associated with antioxidant activity, stress regulation, immune support, and hormonal balance (Marques et al., 2019).

Eleutherococcus senticosus, known as Siberian ginseng, has been widely used in traditional Chinese and Russian medicine, being associated with enhanced physical endurance, improved cognitive performance, and immune health. Its pharmacological activity is attributed to eleutherosides, compounds with promising biological effects (Panossian & Wikman, 2009; Yun, 2015). Currently, both species are widely used in food supplements and herbal preparations, which reinforces the need for stringent quality control practices to prevent misidentification or adulteration.

The growing commercial interest in adaptogenic species such as *R. rosea* and *E. senticosus*, combined with their frequent commercialization in processed forms (powders, capsules, and extracts), has raised significant concerns regarding product authenticity and traceability. Morphological similarities with related species, such as *Rhodiola crenulata*, *Rhodiola sacra*, *Rhodiola kirilowii* or other *Eleutherococcus* species, as well as the indiscriminate use of the term “ginseng,” facilitate both accidental substitution and intentional adulteration. These practices not only compromise product quality but also pose risks to consumer safety, reinforcing the need for stricter control systems and scientific strategies to ensure the botanical identity of plant raw materials.

2.2 *Eleutherococcus senticosus*

E. senticosus, commonly known as Siberian ginseng, belongs to the Araliaceae family and is native to the forests of Siberia, northeastern China, Korea, and Japan (Panossian & Wikman, 2009) (Figures 1 and 2). This deciduous shrub has long been utilized in traditional Chinese and Russian medicine to enhance physical endurance, cognitive function, and immune

response, particularly under conditions of physical or psychological stress (Brekhman & Dardymov, 1969; Davydov & Krikorian, 2000). Traditionally, the root of *E. senticosus* is the primary plant part used for medicinal preparations, being valued for its adaptogenic and tonic properties. In the former Soviet Union, *E. senticosus* was officially adopted as a pharmacological adaptogen and was extensively administered to soldiers, athletes, and cosmonauts to improve stamina, mental clarity, and recovery in extreme environments (Panossian & Wikman, 2009). Due to these adaptogenic properties, the species has gained international recognition and is now incorporated into functional foods, herbal supplements, and pharmaceutical formulations (Kennedy et al., 2001)

Figure 1 - *Eleutherococcus senticosus* (Siberian ginseng) photo: Repina Tatyana © (cc 51696721)

Figure 2 - *Eleutherococcus senticosus* root (Siberian ginseng) photo: Thinkstock

From a phytochemical perspective, *E. senticosus* contains a wide range of bioactive constituents, including eleutherosides (particularly B and E), lignans, flavonoids, phenolic acids, polysaccharides, and triterpene saponins. These compounds are associated with diverse pharmacological effects, such as adaptogenic, immunomodulatory, antioxidant, and neuroprotective activities. Notably, eleutherosides B and E have been employed as chemical markers to evaluate the identity and quality of the species (Graczyk, 2022). Furthermore, the fruits of *E. senticosus* have been reported to contain high levels of polyphenols, flavonoids, and essential minerals, expanding its potential therapeutic applications beyond the traditional use of the roots. The main bioactive compounds identified in *E. senticosus* and their associated pharmacological activities are summarized in Table 1.

Table 1 – Main bioactive compounds identified in *E. senticosus.*

Compound	Chemical class	Main activity
Eleutheroside B	Phenylpropanoid glycoside	Adaptogenic, antioxidant
Eleutheroside E	Lignan glycoside	Immunomodulatory, neuroprotective
Syringaresinol	Lignan	Antioxidant, anti-inflammatory
Isofraxidin	Coumarin	Neuroprotective, antioxidant
Phenolic acids	Phenols	Antioxidant
Polysaccharides	Complex carbohydrates	Immune support

The rapid expansion of the global market for *E. senticosus* based supplements has raised growing concerns regarding product quality and species authenticity. Several studies have reported cases of substitution or adulteration in commercial formulations, either with other *Eleutherococcus* species or with unrelated taxa marketed under the generic label of “ginseng” (Ruhsam, 2018). This issue is exacerbated by the highly processed nature of commercial products, thus limiting the applicability of traditional morphological approaches for taxonomic identification. Ensuring authenticity is therefore a challenge in the commercialization of *E. senticosus*.

To address these challenges, molecular approaches such as DNA barcoding and species-specific PCR have been increasingly applied for the authentication of *E. senticosus*. Maruyama et al. (2010) employed ITS regions of ribosomal DNA and demonstrated that only 70% of the analyzed commercial products contained the correct species, while the remaining samples were composed of mixed or entirely different taxa. Similarly, Ruhsam (2018) examined 25 commercial products and confirmed the presence of *E. senticosus* in all of them, but revealed that 36% also contained DNA from other *Eleutherococcus* species. These findings highlight the

importance of combining molecular identification techniques with quantitative methods, such as real-time qPCR, to detect and quantify adulterants (Hwang, 2015). Moreover, advanced methodologies such as metabarcoding based on next-generation sequencing (NGS) have provided powerful tools for analyzing complex botanical mixtures. Shah et al. (2022), for example, demonstrated that while species-specific PCR detected *E. senticosus* in 22.2% of tested samples, metabarcoding identified it in 55.6%, underscoring the superior sensitivity of NGS-based methods.

From a pharmacological perspective, *E. senticosus* continues to be valued for its adaptogenic, neuroprotective, and immunomodulatory properties. Compounds such as eleutherosides B and E, syringaresinol, and isofraxidin are widely regarded as key markers of biological activity (Chang, 2023). Although chemical quantification techniques provide reliable measures of bioactive content, they are often insufficient for distinguishing between morphologically similar or chemically related species. For this reason, integrating genetic authentication (e.g., PCR and ITS analysis) with phytochemical profiling represents a more robust and comprehensive strategy to ensure both species identity and pharmacological integrity (Maruyama et al., 2010). These considerations underscore the need for continuous research aimed at developing and optimizing reliable identification tools for *E. senticosus*, particularly in light of growing market demand and increasing regulatory scrutiny.

2.3 *Rhodiola rosea*

R. rosea, commonly known as golden root, arctic root, or pink root, belongs to the Crassulaceae family (Figure 3). It is a perennial plant that typically grows in cold regions such as Asia, Northern Europe, Great Britain, and North America, thriving on high-altitude mountain slopes. The species reaches heights of 5 to 40 cm, has a short and thick rhizome, and produces multiple stems. During summer, it blooms with yellow to greenish-yellow flowers, each bearing four sepals and four petals (Bernatoniene et al., 2023). Within the *Rhodiola* genus, more than 200 species have been recognized, but only around 20 are used for medicinal purposes. Among these, *R. alterna*, *R. brevipetiolata*, *R. crenulata*, *R. kirilowii*, *R. quadrifida*, and *R. sacra* are noteworthy, with *R. rosea* being the most extensively studied and widely commercialized.

Figure 3 - *Rhodiola rosea* spp. rosea Photo: Berit Gehrke, UiB.

From a pharmacological perspective, *R. rosea* is often classified as a natural nootropic. According to Malík et al. (2023), its cognitive-enhancing effects are mediated through multiple physiological pathways, often requiring prolonged administration but exhibiting fewer side effects compared to synthetic nootropics. Salidroside, in particular, has demonstrated antioxidant and neuroprotective properties by reducing cytotoxicity, inhibiting intracellular reactive oxygen species (ROS), and modulating apoptosis-related gene expression (Zhu et al., 2021). In PC12 cell culture models, salidroside restored mitochondrial membrane potential and promoted antioxidant enzyme activity in a dose-dependent manner. Animal studies further confirmed its adaptogenic and neuroprotective potential, showing anxiolytic, antidepressant, and mild stimulant effects.

Clinical trials have provided evidence of *R. rosea's* effects in humans. Spasov et al. (2010) demonstrated improvements in physical performance, mental fatigue, neuromotor activity, and overall well-being in international students subjected to exam stress. Additional studies reported reductions in anxiety, stress, anger, confusion, and depressive symptoms among individuals receiving *R. rosea* supplements, though improvements in cognitive performance were not consistently significant. Beyond its neurological applications, *R. rosea* has been associated with improved physical endurance and resilience against exercise-induced fatigue. Its adaptogenic mechanisms involve modulation of the hypothalamic–pituitary–adrenal (HPA) axis, cortisol regulation, nitric oxide signaling, activation of protein kinases such as p-JNK, and stimulation of antioxidant defense proteins (Yao Lu et al., 2022).

Supplementation has also been linked to reduced oxidative stress, lower biomarkers of muscle damage, accelerated recovery, and enhanced athletic performance

The principal bioactive compounds of *R. rosea* and their reported pharmacological activities are summarized in Table 2.

Table 2 – Main bioactive compounds identified in *Rhodiola rosea*

Compound	Category	Primary activities
Salidroside	Phenylethanoid glycoside	Antioxidant, neuroprotective, anti-inflammatory
Rosavin	Cinnamyl alcohol glycoside	Adaptogenic, stress-protective
Rosin	Cinnamyl alcohol glycoside	Antidepressant, nootropic
Rosarin	Cinnamyl alcohol glycoside	Anti-fatigue, mood stabilizer
Tyrosol	Phenol	Antioxidant, cardioprotective

Given its broad pharmacological profile and increasing global demand, *R. rosea* continues to attract scientific and commercial attention as a functional adaptogen. However, the close morphological and phytochemical similarities with related *Rhodiola* species raise significant concerns regarding misidentification and adulteration in commercial products. These challenges highlight the need for reliable and precise authentication methods to ensure the safety, efficacy, and traceability of *R. rosea* derived preparations.

2.4 Botanical authentication of medicinal plants and PFS

In addition to their use in traditional medicine or as Traditional Herbal Medicinal Products (THMP), an increasing number of medicinal plants are incorporated into formulations marketed as food supplements. Plant food supplements (PFS) have shown rapid global growth, driven by consumer preference for healthier lifestyles, the perception that natural products are safer, dissatisfaction with synthetic drugs, and rising healthcare costs (El-Ahmady et al., 2016; Sasikumar, 2016; Garcia-Alvarez et al., 2014). The herbal supplement market is currently estimated to exceed USD 7.4 billion annually in the United States and approximately €1.8 billion in the European Union (Frigerio et al., 2021).

Dietary supplements, including botanically derived formulations, are regulated as food products under both U.S. law (Dietary Supplement Health and Education Act) and European law (Directive 2002/46/EC). Consequently, they do not require pre-market authorization, leaving manufacturers solely responsible for ensuring product safety and compliance (Moraes et al., 2015). Despite safety frameworks such as Good Manufacturing Practices (FDA, 2007) and Good

Agricultural and Collection Practices, significant concerns remain regarding the quality and authenticity of these products.

Adulteration of herbal supplements is a widespread problem, involving either the deliberate substitution of high-value species with cheaper or morphologically similar plants or the addition of pharmaceutical compounds to enhance efficacy (Rocha et al., 2016; Amidžić et al., 2023). Misidentification may also occur when wild-harvested material lacks proper taxonomic verification (Grazina et al., 2020). The globalization of supply chains amplifies these risks by increasing the complexity of sourcing, production, and distribution networks, thereby facilitating both inadvertent substitutions and intentional fraud at different stages (Grazina et al., 2020; Liu et al., 2022). Moreover, growing consumer demand exerts pressure on raw material availability, creating further incentives for fraudulent practices during periods of scarcity.

Ensuring authenticity requires robust species authentication strategies across all stages of production, from raw plant material to finished formulations. A variety of analytical methods can be employed, including morphological, chemical, and genetic approaches (Raclariu et al., 2018). The choice of method depends on factors such as the species involved, the degree of processing, and the complexity of the formulation. While macroscopic and microscopic analyses are cost-effective for raw materials, they are unsuitable for processed powders or extracts (Heubl et al., 2010). Phytochemical profiling through chromatographic techniques such as HPLC and TLC can identify metabolites and chemical markers, yet variability due to environmental and physiological factors, coupled with the need for extensive authenticated reference material, limits their reliability (Grazina et al., 2023; Wang et al., 2014).

DNA-based methods are generally considered more robust for species-level authentication, particularly in processed samples where morphological features and chemical signatures are less reliable. DNA remains stable across diverse conditions, and molecular techniques provide high specificity and reproducibility (Franz et al., 2011; Costa et al., 2015). **Table 3** summarizes the main authentication methods for medicinal plants and PFS, highlighting their applicability, strengths, and limitations according to the sample type and condition.

Table 3 – Overview of authentication methods for medicinal plants and PFS.

Method	Type	Sample Suitability	Main Advantages	Main Limitations
Macroscopic analysis	Morphological	Whole plants, raw material	Fast, inexpensive	Not suitable for powders or extracts
Microscopic analysis	Morphological	Powders, fragments	Detects inorganic fillers, tissue structures	Limited with heavily processed samples
Phytochemical profiling (HPLC, TLC, MS)	Chemical	Extracts, raw or semi-processed material	Identifies metabolites, chemical markers	Variability due to environmental factors; requires reference standards
Chromatographic fingerprinting	Chemical	Extracts, complex formulations	Detects overall profile of compounds	Difficult to link to specific species
DNA barcoding	Molecular	Raw, semi-processed materials	High taxonomic resolution; universal primers	May not work with degraded DNA
DNA metabarcoding (NGS)	Molecular	Complex mixtures, processed products	Identifies multiple species simultaneously	High cost, complex data analysis
Species-specific PCR	Molecular	Extracts, supplements	Fast, highly specific for known targets	Requires prior knowledge of adulterants
PCR- HRM	Molecular	Complex or processed samples	High sensitivity; useful for detecting minor components	Requires careful assay optimization

Several identification techniques currently used for botanical authentication have their roots in pharmacognosy, a scientific discipline that for centuries has focused on the study of medicinal plants, including their characterization and quality control. Each method employs distinct principles and requires varying levels of prior information. Traditionally, pharmacopoeias have relied on macroscopic and microscopic features, simple chemical assays, and, more recently, chemical “fingerprinting” techniques to establish a plant's identity (Smillie et al., 2010). To overcome limitations of these approaches, advanced methods have been developed, including molecular tools based on DNA analysis, which offer greater precision and applicability across diverse sample types.

Several molecular approaches have already been implemented for botanical authentication. Species-specific techniques allow targeted detection of known adulterants (Grazina et al., 2020). In contrast, universal approaches such as DNA barcoding and

metabarcoding, utilizing high-throughput sequencing such as next generation sequencing (NGS), are more suitable when unknown species are involved (Soares et al., 2015). Nonetheless, efficient DNA extraction remains a critical factor, particularly for highly processed commercial formulations (Costa et al., 2015).

Beyond their scientific utility, authentication techniques are also essential from a regulatory perspective. Accurate identification of plant species in commercial products is a critical requirement for ensuring quality, safety, and efficacy, as adulteration or misidentification may compromise therapeutic activity and pose risks to consumer health (Raclariu et al., 2018). Regulatory agencies in both Europe and North America increasingly emphasize the implementation of rigorous quality control measures, highlighting the relevance of authentication protocols across the entire supply chain.

Recent technological advances have significantly expanded the range of available tools. DNA barcoding, metabarcoding with next-generation sequencing (NGS), and high-throughput metabolomic profiling now allow simultaneous identification of multiple taxa within complex mixtures, providing unprecedented resolution in authenticity testing (Shah et al., 2022). These approaches are particularly useful in detecting hidden adulteration and tracing raw material origins. At the same time, DNA-based methods, including PCR, qPCR, and high-resolution melting (HRM) analysis, have emerged as rapid, highly specific, and reproducible techniques for distinguishing between closely related medicinal species, even in extracts or commercial supplements (Costa et al., 2015).

Despite these advances, several challenges remain. DNA degradation in highly processed products can limit molecular approaches, while the lack of comprehensive reference databases for both genetic markers and chemical profiles hinders universal application (Costa et al., 2015). Moreover, technical optimization such as efficient DNA extraction and assay validation remains necessary to ensure reproducibility across laboratories. For these reasons, continuous methodological development and cross-validation are crucial to advancing the field of botanical authentication.

Among molecular tools, PCR-based approaches using species-specific primers, real-time PCR, and HRM analysis, stand out as particularly powerful strategies for ensuring authenticity of high-value medicinal plants such as *R. rosea* and *E. senticosus*. These methodologies form the basis of the analytical framework applied in the present work,

providing a reliable and reproducible platform to detect adulteration and guarantee product traceability.

2.5 Chemical techniques: chromatographic analyses

Chemical analytical techniques that include a separation step are widely applied in the authentication of botanical products. Among them, high-performance liquid chromatography (HPLC), capillary electrophoresis (CE), and gas chromatography (GC) are commonly used. HPLC, in particular, is considered one of the most versatile techniques, as it is suitable for thermolabile phytochemicals and can be coupled with various detectors, such as diode-array detectors (DAD) and mass spectrometry (MS). The combination of liquid chromatography with mass spectrometry (LC-MS) has emerged as one of the most powerful tools for botanical authentication due to its high sensitivity, resolution, accuracy, and reproducibility (Grazina et al., 2023).

Two main analytical approaches can be employed with LC-MS: targeted and untargeted profiling. In targeted analysis, the chemical composition of the plant is already characterized, and specific marker compounds have been established for that species. The aim is to detect and quantify these markers with high sensitivity and selectivity (Grazina et al., 2023). However, the number of metabolites unique to a single species is often limited, and therefore a combination of several markers is typically required to obtain a representative and reliable chemical profile. Targeted analyses rely on the quantitative measurement of these markers, which in turn requires the availability of certified reference standards.

Untargeted profiling, in contrast, does not depend on predefined markers. Instead, it aims to capture as many compounds as possible to generate a comprehensive "chemical fingerprint" of the sample. Unknown metabolites may be identified or structurally characterized through high-resolution mass spectrometry (HR-MS), but the primary goal is not full structural elucidation; rather, it is to compare the generated fingerprint against a library of authenticated reference samples. Since untargeted methods generate large and complex datasets, advanced chemometric approaches such as hierarchical cluster analysis (HCA) and principal component analysis (PCA) are frequently applied to classify and discriminate samples based on similarities or differences in their chemical profiles.

One of the major challenges in LC-MS-based profiling whether targeted or untargeted is the intrinsic variability in plant chemical composition. Environmental factors such as climate, soil type, harvest time, and post-harvest processing strongly influence metabolite

content, complicating the establishment of standardized chemical markers. For this reason, the development of statistically robust and reproducible chemical fingerprints requires a sufficiently large set of authenticated reference samples to define the acceptable range of variability.

The careful selection of health-relevant and species-specific chemical markers, ideally in combination with multiple compounds, significantly reduces the risk of adulteration or misidentification. Nevertheless, limitations persist, particularly the availability of high-quality reference standards and the need for validated analytical performance criteria. Thus, while chromatographic and mass spectrometric techniques provide valuable chemical insights, their limitations underscore the complementary role of molecular approaches in ensuring accurate botanical authentication. (Smillie et al., 2010).

2.6 DNA based approaches

2.6.1 Genetic markers – Loci

Selecting suitable loci for plant barcoding presents particular challenges, as plant genomes generally evolve more slowly than those of animals, resulting in lower levels of sequence divergence (Hollingsworth et al., 2009). An ideal barcode locus must combine universality of primers, high amplification success, and sufficient discriminatory power to distinguish closely related taxa (Purushothaman et al., 2014). Over the past two decades, several genomic regions have been investigated as potential plant barcodes, including plastid genes (matK, rbcL), nuclear ribosomal DNA regions (ITS1, ITS2), and intergenic spacers such as trnH-psbA.

The Consortium for the Barcode of Life (CBOL) Plant Working Group recommended the combined use of matK and rbcL as the standard "core barcode" for plants (Little et al., 2013). The matK gene provides relatively high discriminatory power due to its elevated substitution rates but often suffers from inconsistent amplification across taxa. Conversely, rbcL is highly universal and exhibits robust amplification, although its discriminatory capacity is lower at the species level. When combined, these loci balance universality and resolution, offering improved identification performance).

Nuclear ribosomal regions, particularly ITS and ITS2, have been extensively employed as complementary loci because of their high interspecific variability and strong phylogenetic resolution (Chen et al., 2010; Michel et al., 2016). The ITS2 region, in particular,

has demonstrated excellent amplification efficiency and species-level discrimination across diverse plant families, making it one of the most effective loci for medicinal plant authentication (Yao et al., 2010; Cheng et al., 2015).

Despite these advances, no single locus universally satisfies all criteria for plant barcoding. Consequently, *multilocus* approaches are generally required, often combining plastid and nuclear regions to achieve both amplification reliability and high discriminatory power. This *multilocus* framework has become especially relevant in the authentication of herbal medicines and plant food supplements, where accurate discrimination among closely related species is critical for ensuring quality, safety, and regulatory compliance.

2.6.2 DNA Barcoding

The concept of DNA barcoding refers to the use of short, standardized DNA sequences as molecular identifiers to distinguish species. First introduced by Hebert et al. (2003), this approach has proven particularly valuable in cases where morphological identification is difficult, subjective, or error-prone. DNA barcodes are typically obtained from conserved genomic regions, such as mitochondrial, nuclear, or plastid genes (Selvaraj et al., 2013).

For animals, the mitochondrial gene cytochrome c oxidase subunit 1 (COI) is the most widely used barcode because of its high interspecific variability. However, in plants, mitochondrial genes evolve more slowly and show limited variability, making them less effective for species-level discrimination. Instead, plastid and nuclear regions with higher substitution rates have been proposed as more suitable barcodes. Among these, the plastid genes rbcL and matK are the most frequently applied, and their combination has been recommended by the Consortium for the Barcode of Life (CBOL) as the “core barcode” for land plants. Nuclear regions such as the internal transcribed spacer (ITS1/ITS2) have also been widely used as complementary loci to increase resolution (Parveen et al., 2016; Mishra, 2016).

Although DNA barcoding enables accurate identification even in highly processed materials, its performance depends heavily on the choice of loci and the availability of comprehensive and curated reference databases. Limitations include insufficient interspecific variation in some plant groups, difficulties caused by hybridization or polyploidy, and challenges in obtaining amplifiable DNA from degraded samples, such as those found in processed herbal supplements.

Despite these limitations, DNA barcoding remains a cornerstone of molecular

authentication, offering a standardized and broadly applicable framework for species identification. When combined with complementary approaches such as quantitative PCR, high-resolution melting (HRM), or next-generation sequencing (NGS)-based metabarcoding, it provides a powerful platform for ensuring the authenticity of medicinal plants and plant-derived supplements.

2.6.3 PCR and real-time PCR

The polymerase chain reaction (PCR) is a cornerstone molecular technique that enables the amplification of specific DNA fragments, providing the basis for numerous molecular authentication methods (Zhu et al., 2020). Several PCR-based fingerprinting techniques—including random amplified polymorphic DNA (RAPD), sequence-characterized amplified region (SCAR), directed amplification of minisatellite-region DNA (DAMD), and simple sequence repeats (SSR)—have been successfully applied to differentiate closely related plant species and detect adulteration in herbal products (Paran et al., 1993; Xue et al., 2008). These approaches are particularly valuable for distinguishing species with high morphological similarity or overlapping phytochemical profiles, where classical methods are insufficient.

Real-time PCR represents a major advancement over conventional PCR, as it enables the quantification of DNA during amplification while also improving specificity through the use of fluorescent dyes or sequence-specific probes (Navarro et al., 2015). This method combines sensitivity, speed, and reproducibility, making it particularly suitable for diagnostic and food analysis applications. In the context of botanical authentication, real time PCR is especially effective when adulterant species are known and target-specific primers or probes can be designed to detect them with high precision (Wu et al., 2015).

In addition to single-target assays, multiplex real-time PCR protocols have been developed to simultaneously identify and quantify multiple plant species within complex formulations. Doganay et al. (2018) demonstrated the utility of this technique for authenticating herbal mixtures, showing that the technique remained effective even when only trace amounts of DNA were available. This highlights its potential as a reliable quality control tool for the authentication of commercial herbal products. However, despite its numerous advantages, it also presents limitations. It requires prior knowledge of target sequences, making it less effective when adulterants are unknown. Furthermore, DNA degradation in processed materials may reduce amplification efficiency, and careful assay optimization is

necessary to avoid false negatives or quantification errors. Nevertheless, PCR and real time PCR remain among the most powerful and widely applied tools for plant authentication, providing a robust foundation for more advanced molecular techniques such as high-resolution melting (HRM) analysis and next-generation sequencing (NGS).

2.6.4 High-resolution melting (HRM)

High-resolution melting (HRM) analysis is a post-PCR technique that detects variations in DNA sequences by analyzing the melting behavior of double-stranded DNA (Costa et al., 2016). During HRM, fluorescent dyes intercalate into double-stranded DNA, and as the temperature increases, changes in fluorescence reflect the dissociation or "*melting*" profile of the DNA. Differences in sequence, fragment length, and GC content influence the melting curve, allowing the discrimination of even single-nucleotide polymorphisms (Wittwer et al., 2003; Herrmann et al., 2016).

One of the main advantages of HRM is its speed and cost-effectiveness. The method requires no post-PCR processing steps, thereby reducing contamination risks and laboratory workload. The use of saturating fluorescent dyes such as *EvaGreen* ensures high sensitivity and reproducibility while avoiding inhibition of polymerase activity (Vossen et al., 2009). These characteristics make HRM particularly suitable for high-throughput applications in the authentication of botanical products.

HRM has been shown to be highly effective in the analysis of processed and complex matrices, such as powdered herbal materials and dietary supplements, where traditional morphological or chemical methods are not applicable. By targeting species-specific DNA fragments, HRM can distinguish authentic species from closely related adulterants, even when present in small proportions. This makes it a valuable tool for ensuring product quality and traceability in commercial herbal preparations.

A notable development in this field is the integration of HRM with DNA barcoding, known as Bar-HRM. This hybrid approach combines the universality of DNA barcodes with the discriminatory power of HRM analysis, enabling rapid and accurate species identification as well as adulteration detection in complex herbal formulations (Sun et al., 2016). Given its sensitivity, low cost, and applicability to routine testing, HRM and Bar-HRM are increasingly recognized as essential tools in the quality control of herbal medicines, food products, and pharmaceuticals.

2.6.5 Next generation sequencing

Advancements in sequencing technologies have revolutionized molecular approaches for botanical authentication, particularly through the application of DNA metabarcoding using next-generation sequencing (NGS). This method enables the simultaneous identification of multiple taxa in complex mixtures, making it especially suitable for analyzing herbal supplements, which often contain processed or multi-ingredient formulations (Smillie et al., 2010). NGS platforms such as Roche 454, Ion Torrent, and Illumina MiSeq can generate large volumes of sequencing data from mixed DNA templates, thereby allowing the detection of multiple plant species within a single assay (Shokralla et al., 2012; Kircher et al., 2010).

The selection of appropriate DNA markers is a critical determinant of success. Loci such as ITS2 and trnL have been widely employed, as demonstrated in studies analyzing Traditional Chinese Medicine formulations, where DNA metabarcoding revealed both intended species and undeclared adulterants (Coghlan et al., 2012; Cheng et al., 2014). Recent work has shown that Ion Torrent and Illumina platforms are effective for supplement authentication, with Illumina's higher throughput and sequence accuracy making it particularly suitable for multi-locus metabarcoding approaches (Staats et al., 2017).

NGS provides several advantages over conventional barcoding, including high sensitivity and high throughput. This is particularly relevant for processed botanical products, where traditional morphological or chemical methods are ineffective. Furthermore, multi-locus metabarcoding approaches expand taxonomic resolution and allow the detection of both major and trace-level species within complex mixtures.

Despite these strengths, NGS-based approaches also face important limitations. The lack of universal plant barcodes reduces consistency across studies, and the construction of comprehensive, curated reference databases remains an ongoing challenge (Staats et al., 2016). In addition, bioinformatic pipelines for sequence filtering, clustering, and taxonomic assignment are complex and require careful standardization to avoid false positives or misidentifications (Haynes et al., 2019; Raclariu et al., 2018).

Taken together, NGS has become a powerful tool in the field of botanical authentication, offering unprecedented resolution in detecting adulteration and substitution in commercial herbal products. However, its successful implementation requires not only optimized laboratory protocols but also robust reference databases and bioinformatics

frameworks. As sequencing technologies continue to advance, NGS is expected to play an increasingly central role in ensuring the quality, safety, and traceability of botanical supplements.

2.6.6 Authentication of target species: *E. senticosus* and *R. rosea*

The authentication of high-value medicinal plants has become a central concern in the field of phytotherapy, particularly for adaptogenic species such as *E. senticosus* (Siberian ginseng) and *R. rosea* (golden root). Both species are widely commercialized in dietary supplements and herbal products, but their popularity, combined with morphological similarity to related taxa and increasing global demand, has made them frequent targets of substitution and adulteration (Booker et al., 2016; Ma et al., 2021). Ensuring authenticity is therefore crucial not only for regulatory compliance but also for consumer safety and therapeutic efficacy.

For *E. senticosus*, adulteration typically involves substitution with other *Eleutherococcus* species or unrelated plants such as *Periploca sepium* and *Codonopsis pilosula* (Sun et al., 2015). Chemotaxonomic methods based on HPLC, TLC, and UPLC have been applied to detect eleutherosides B and E, recognized as chemical markers of the species (Panossian et al., 2010; Ma et al., 2011). However, significant variability in compound levels has been observed in commercial products, often indicating adulteration or poor standardization (Booker et al., 2016). DNA-based methods have therefore gained prominence, with studies demonstrating the utility of ITS2 barcoding for species identification (Ruhsam et al., 2018; Ivanova et al., 2016). Nonetheless, challenges such as degraded DNA in processed products and PCR inhibition remain. More recent approaches, including qPCR with species-specific primers (Kim et al., 2020) and HRM analysis (Chen et al., 2019), have shown promise in improving sensitivity and specificity.

In the case of *R. rosea*, the main challenge lies in its close morphological similarity with other *Rhodiola* species, such as *R. crenulata*, *R. kirilowii*, and *R. serrata*, which often leads to substitution in the marketplace (Marchev, 2020; Ma et al., 2021). Chemical fingerprinting approaches, such as UHPLC-DAD combined with H-NMR and pattern recognition, have been employed to differentiate *Rhodiola* species, with variable results among commercial samples (Ma et al., 2021; Marchev et al., 2020). Investigations using HPTLC, MS, and H-NMR revealed that up to 40% of commercial products were inconsistent with authentic *R. rosea* profiles, and in some cases contained no *Rhodiola* material at all

(Booker et al., 2015). DNA-based strategies, particularly ITS2 barcoding, have also been applied, though difficulties in amplifying DNA from extracts limit their universal application (Ruhsam et al., 2018; Xin et al., 2015). These studies confirm widespread substitution with other *Rhodiola* species and highlight the need for more sensitive molecular approaches.

Taken together, these findings emphasize that both *E. senticosus* and *R. rosea* face similar authentication challenges, with adulteration driven by high demand, morphological similarity to related species, and variability in chemical composition. While chemotaxonomic methods remain useful, molecular tools such as species-specific qPCR and HRM analysis offer greater resolution and applicability to processed products. These integrated strategies provide a reliable framework for ensuring the authenticity of adaptogenic plants and represent the methodological basis applied in the present work.

3. MATERIALS AND METHODS

3.1 Sample Collection and Characterization

Samples of *Rhodiola spp*. and *Eleutherococcus spp*. were obtained from botanical gardens (B.G.), commercial suppliers, online markets, and reference collections to reflect the diversity and heterogeneity of plant materials available in research and trade. Each item was classified by (i) declared species, (ii) matrix (whole plant, root, powder, seed, or extracted DNA), and (iii) source (institution/brand, country). Voucher IDs or lot numbers were recorded when available (Tables 4 and 5).

To ensure the authenticity of the reference material used for primer optimization and HRM calibration, one Rhodiola rosea specimen (R04, whole plant – Botanical Garden Berlin, BGBM) was subjected to ITS2 metabarcoding of the nuclear ribosomal ITS2 region. The obtained sequence was identified as *R. rosea* based on BLASTn comparison with GenBank reference sequences, confirming its taxonomic identity. This verified specimen was subsequently employed as the reference control for all optimization and validation assays described in Section 4.3.

Table 4 - Species identification, sample type, and origin of selected *Rhodiola* specimens used in this study.

ID	Species	Sample Type	Origin
R1	*R. rosea*	Root	Traditional herbal store (commercial)
R2	*R. rosea*	Powder	Biosamara (commercial)
R3	*R. rosea*	Seed	Algar Sementes (commercial)
R4	*R. rosea*	Whole plant	B.G. Berlin (BGBM)
R5	*Rhodiola rosea*	Powder	SaludViva (commercial)
R6	*R. heterodonta*	Whole plant	B.G. Bonn - Germany
R7	*R. rosea*	Plant with fungi	B.G. Bonn - Germany
R8	*R. rosea*	Whole plant	B.G. Oulu - Finland
R9	*R. rosea*	Whole plant	B.G. COI – Coimbra - Portugal
R10	*R. porterbaw*	Whole plant	B.G. Edinburgh - Scotland
R11	*R. crenulata*	Whole plant	B.G. Edinburgh - Scotland
R12	*R. rosea*	Whole plant	B.G. Edinburgh - Scotland
R13	*R. rosea*	Root	Etsy (commercial)
R14	*Rhodiola sp.*	Root	Etsy (commercial)
R15	*R. rosea*	Root	Etsy (commercial)
R16	*R. bupleuroides*	Root	Etsy (commercial)
R17	*R. rosea*	Powder	Etsy (commercial)
R18	*R. stephanii*	Root	Gorna Oryakhovitsa (commercial, Bulgaria)
R19	*R. kirilowii*	Whole plant	Bergius Botanic Garden - Sweeden

Table 4 (cont.)

ID	Species	Sample Type	Origin
R20	*R. yunnanensis*	Whole plant	B.G. Berlin (BGBM) - Germany
R21	*R. rosea*	Whole plant	B.G. Edinburgh - Scotland
R22	*R. pachyclados*	Whole plant	B.G. Edinburgh - Scotland
R23	*R. kirilowii*	Whole plant	B.G. Edinburgh - Scotland
R24	*Rhodiola sp.*	Whole plant	B.G. Oulu -Finland
R25	*R. rosea*	Whole plant	B.G. Berlin (BGBM) - Germany
R26	*R. rosea*	Whole plant	B.G. Edinburgh - Scotland
R27	*R. crenulata*	Whole plant	B.G. Berlin (BGBM) - Germany
R28	*R. crenulata*	DNA	B.G. Kew – UK
R29	*R. yunnanensis*	DNA	B.G. Kew – UK
R30	*R. rosea*	DNA	B.G. Kew – UK
R31	*R. rosea*	Whole plant	B.G. Edinburgh - Scotland
R32	*R. rosea*	Whole plant	B.G. Berlin (BGBM) - Germany
R33	*R. rosea*	Whole plant	B.G. Edinburgh - Scotland
R34	*R. rosea*	Whole plant	B.G. Edinburgh - Scotland
R35	*R. rosea*	Whole plant	B.G. Edinburgh - Scotland

Table 5 - Species identification, sample type, and origin of selected *Eleutherococcus* specimens used in this study.

ID	Species	Sample Type	Origin
E1	*E. leucorrhizus*	Plant	B.G. Edinburgh
E2	*E. lasiogyne*	Plant	B.G. Edinburgh
E3	*E. lasiogyne*	Plant	B.G. Edinburgh
E4	*E. lasiogyne*	Plant	B.G. Edinburgh
E5	*E. henryi*	Plant	B.G. Edinburgh
E6	*E. senticosus*	Plant	B.G. Edinburgh
E7	*E. leucorrhizus*	Plant	B.G. Edinburgh
E8	*E. leucorrhizus*	Plant	B.G. Edinburgh
E9	*E. leucorrhizus*	Plant	B.G. Edinburgh
E10	*E. leucorrhizus*	Plant	B.G. Edinburgh
E11	*E. divaricatus*	Plant	B.G. Edinburgh
E12	*E. henryi*	Plant	B.G. Edinburgh
P154	*E. senticosus*	Root	Celeiro PT (commercial)

* Pfaffia glomerata (Brazilian ginseng) was used as a quality control in the cross-amplification assays

3.2 Commercial samples of *E. senticosus*

For processed supplements declaring *E. senticosus* (Table 6), an adapted extraction was employed to mitigate inhibitors typical of complex matrices: 50 mg of material were lysed in PL1 supplemented with 1% (w/v) PVPP, RNase A added post-lysis, incubation extended to 30–60 min at 65 °C, and an additional PW2 wash was included before elution. Where

necessary, an inhibitor-removal step, was applied. Extracts were then analyzed by species-specific PCR and HRM.

Table 6 - Commercial food supplements containing *E. senticosus* declared as ingredient

ID	Brand	Product	Presentation Type	Declared Composition
S1	Integralia	Eleuterococo Extracto	Plastic bottle with capsules	*Eleutherococcus senticosus*
S2	Soria Natural	Eleuterococo 15-S	Box with capsules	*Eleutherococcus senticosus* (Siberian ginseng)
S3	Integralia	Eleuterococo Forte Ecológico	Box with capsules	*Eleutherococcus senticosus*
S4	Integralia	Eleuterococo Complex	Box with capsules	*Eleutherococcus senticosus*

Table 7 - Shows the commercial herbal products labeled as containing *E. senticosus* used in this study.

ID	Product	Presentation Type	Declared Composition
Sg1	Chá Flora Mundial	Root	*E. senticosus*
Sg2	La flor del Pirineo	Root	*E. senticosus*
Sg3	Siberian Gingensg Root	Root	*E. senticosus*
Sg4	Siberian Gingensg powder	Powder	*E. senticosus*
Sg5	Gram Velada S.L	Powder	*E. senticosus*
Sg6	Chasgormet	Powder	*E. senticosus*
Sg7	Treasures Herbal	Powder	*E. senticosus*

The extracted DNA was then subjected to species-specific PCR and HRM analysis as described in subsequent sections. The inclusion of commercial supplements was intended to assess the robustness and practical applicability of the molecular authentication methods, particularly in detecting adulteration or substitution in consumer-ready formulations.

3.3 Sample preparation and storage

The plant samples listed in Tables 4 and 5, were obtained from two primary sources: botanical gardens and commercial suppliers. Specimens collected from botanical gardens were obtained with proper identification to ensure taxonomic accuracy. Commercial samples, including roots and powders, were sourced from herbal stores and online marketplaces. Upon receipt, samples were stored in labeled paper envelopes with silica gel at room temperature, separated by species to prevent cross-contamination. Before extraction, approximately 50 mg

were transferred to 2 mL. Work surfaces and tools were sterilized or cleaned with ethanol 70% between samples. The commercial samples were ground into powder using a commercial blender (Moulinex). Between grindings, the lid, container, and blade were immersed in a diluted bleach solution, thoroughly rinsed with distilled water, and dried in an oven to avoid cross-contamination.

3.4 DNA Extraction and Quantification

Genomic DNA was extracted using the NucleoSpin® Plant II Kit (Macherey-Nagel) following the manufacturer's protocol with minor modifications. Approximately 50 mg of plant's tissue or powdered commercial samples were transferred to a 2 mL screw-cap tubes containing two 3 mm zirconia beads, homogenized (Precellys, 6200 rpm, 3×5 s) and lysed in 400 µL of Buffer PL1 at 65 °C for 60 min. RNase A (10 µL) was added, and samples were mixed by vortexing. Lysates were clarified using NucleoSpin® Filters by centrifugation at 11,000 × g for 2 min, and the flow-through was mixed with 450 µL of Buffer PC to promote DNA binding. The mixture was loaded onto NucleoSpin® Plant II silica columns in successive aliquots and centrifuged at 11,000 × g for 1 min. Columns were washed with 400 µL of PW1, followed by 700 µL of PW2 and an additional 200 µL PW2 wash, centrifuged for 2 min to fully dry the membrane. DNA was eluted in 50 µL of pre-heated Buffer PE (65 °C), incubated for 5 min and centrifuged at 11,000 × g for 1 min. Eluted DNA was stored at –20 °C until use.

DNA concentration and purity were determined in triplicate using a SPECTROstar Nano spectrophotometer. Absorbance ratios A260/A280 and A260/A230 were recorded to assess protein and polysaccharide/polyphenol carry-over, respectively. Only extracts with A260/A280 values between 1.4 and 2.0 were selected for downstream assays, as these ratios are associated with optimal performance in PCR-based applications (Schrader et al., 2012). All samples were normalized to 10 ng/µL prior to molecular analyses.

3.5 Primer Design

Species-specific primers were designed to selectively amplify unique genomic regions of *R. rosea* and *E. senticosus*, with the purpose of enabling their molecular discrimination from the most frequently reported adulterant species. In addition, primers were also designed aiming for HRM analysis. Candidate loci were identified by retrieving sequences from public

repositories, GenBank (NCBI), which are widely recognized resources for molecular taxonomy and authentication studies (Hollingsworth et al., 2009; Chen et al., 2010).

Primer design was manually conducted using *BioEdit* or the NCBI primerblast tool, applying parameters considered critical for downstream molecular assays. Amplicon sizes were restricted to 100–300 bp, a range previously reported as optimal for degraded DNA and for real-time PCR and HRM assays, balancing amplification efficiency, sensitivity, and melting curve resolution (Costa et al., 2015; Grazina et al., 2023). Primer length was preferentially between 18-24 bp and GC content between 40-60%. Regions showing high interspecific variability but minimal intraspecific polymorphism were prioritized to maximize discriminatory power. For HRM analysis, species sequences were aligned and primers manually designed to target conserved flanking regions while placing the sequence variations near the centre of the amplicon.

The specificity (for species and for genus in the case of HRM) of the designed primers was assessed through *Primer-BLAST* (NCBI), which ensured the absence of significant homology with non-target taxa. Thermodynamic properties, including GC content, self-complementarity, and the likelihood of primer–dimer formation, were further evaluated with *OligoAnalyzer* (IDT) to guarantee structural stability and efficient amplification (Untergasser et al., 2012).

All primers were synthesized by *STAB VIDA* – Investigação e Serviços em Ciências Biológicas, Lda., and tested first by conventional PCR, followed by real-time PCR coupled with HRM when applicable. Validation criteria included consistent amplification of the expected fragment size, absence of non-specific products as verified by agarose gel electrophoresis and, in the case of HRM, the generation of distinct melting profiles that enabled clear differentiation between the targeted species and others.

Table 8 presents the primer sequences designed for *R. rosea*, while Table 8 summarizes those developed for *E. senticosus*. These primers formed the basis for subsequent PCR and HRM assays applied in the present study to assess species authenticity in both reference samples and commercial supplements.

Table 8 – Species-specific primers designed for the molecular authentication of *Rhodiola rosea.*

Primer Name	Sequence (5'→3')	Length (bp)	Amplicon length (bp)	
RodR2-F	TTGCGCTCGTTGCTGAT	17	104	
RodR2-R	CCCTGGCAACCCAAGAT	17		141
RodR3-F	GTACTCCATTTGCCTTCCC	19		
Rd-HRM1-F	AAACGAATGAACCCCGGC	18	124	
Rd-HRM1-R1	TTGCCGAGAGTCGTTATGG	19		
Rd-HRM2-F	TGCGCCCGAAGCCATTAG	18	116	
Rd-HRM2-R	CATCCGCGAGTTTGGGCT	18		

Table 9 – Species-specific primers designed for the molecular authentication of *E. senticosus.*

Primer Name	Sequence (5'→3')	Length (bp)	Amplicon length (bp)
EleHRM-F	CTGAGGGGCGGATACTGG	18	162
EleHRM-R	ACGGCACAACAGGGTCACAT	20	
Esent1-F2	GGTGAACCTGCGGAAGGAT	19	119
Esent1-R2	GACAATGGGTTCGCGACTTGG	21	
EsentFDS-F	AAGATCATCCGAGCCAAGCG	20	129
EsentFDS-R	TGTCCAGGCAAGGCTTCAAA	20	
EsentBAS2-F	TGGCCATTCAACAAGTTGCG	20	136
EsentBAS2-R	TCTCTGCCCACCAACACATC	20	
EsentCYP-F	CCGGCTGGAAATACTGGTGT	20	143
EsentCYP-R	AGGCTTTGTGAGGGAACAGG	20	
EleuFDS-F	CACTCTCAAGCTTCAGGATGT	21	282
EleuFDS-R	GTAAATGCAACCCCTTCATATTG	23	

3.6 Cross-Reactivity Testing

The specificity and robustness of the molecular authentication system were evaluated through a cross-reactivity assay. This validation step is fundamental in authentication studies as it ensures that the developed primers selectively detect the target species and are not affected by the presence of DNA from non-target botanical components.

Methodological validation requires demonstrating that species-specific primers consistently amplify only the intended organism and do not generate false positives when exposed to DNA from common contaminants, adulterants, or phylogenetically related taxa. The mixtures used in the cross-reactivity assays were prepared from DNA isolated from authenticated plant species, which had been previously authenticated by ITS2 metabarcoding. A total of 52 different species traditionally used for brain health were evaluated for cross-

reactivity of *E. senticosus* primers, while mixtures comprising a total of 43 species were used for *R. rosea*. The complete list of plant species included in the preparation of these mixtures is provided in Annex A.

3.7 Conventional PCR Conditions

Polymerase chain reaction (PCR) amplifications were performed in a final reaction volume of 10 µL, consisting of 5 µL of Q5® High-Fidelity 2X Master Mix (2×, New England Biolabs), 0.5 µL of each primer (10 µM), 3 µL of ultrapure nuclease-free water, and 1 µL of genomic DNA (10 ng/µL).

The thermal cycling program was carried out in a T100 Thermal Cycler (Bio-Rad) and comprised the following steps: an initial denaturation at 98 °C for 3 min, followed by 39 amplification cycles of denaturation at 98 °C for 30 s, annealing at the temperature specified for each primer pair in Table 9 for 30 s, and extension at 72 °C for 30 s. A final elongation step was performed at 72 °C for 5 min to ensure complete extension of amplicons. Amplicons were subsequently stored at 4 °C until electrophoretic evaluation.

Table 10 – Universal plant DNA barcoding primers and optimized PCR conditions.

Primer	Sequence (5'→3')	Amplicon size (bp)	Annealing temp (°C)	Reference
ITS-S2F	ATGCGATACTTGGTGTGAAT	~420	55	Chen et al. 2010
ITS-S4R	TCCTCCGCTTATTGATATGC			
rbcLa-F	ATGTCACCACAAACAGAGACTAAAGC	~600	58	Kress & Erickson (2007)
rbcLa-R	GTAAAATCAAGTCCACCRCG			

For species authentication, each designed primer pair (Table 8 and 9) was tested using a gradient of temperatures to establish the optimum temperature of annealing.

3.8 Agarose Gel Electrophoresis

PCR products were evaluated by horizontal agarose gel electrophoresis to confirm amplification and assess fragment size. Gels were prepared at a final concentration of 1% (w/v) agarose in 1× TAE buffer (89 mM Tris-borate, 2 mM EDTA, pH 8.3), and stained with GelRed® (Biotium) for DNA visualization under UV light.

For each reaction, 2 µL of PCR product was mixed with 2 µL of 6× loading buffer and loaded into the wells. A 100 bp DNA ladder (New England Biolabs) was included in each run as a molecular size marker. Electrophoresis was performed at a constant voltage of 85 V for 40 minutes.

Following separation, gels were visualized and recorded using a GelDoc™ XR+ Imaging System (Bio-Rad). Amplicons were considered specific when single, well-defined bands of the expected size were observed, without secondary or non-specific amplification products. Representative gel images are presented in the Results section.

3.9 Real time PCR coupled with High-Resolution Melting (HRM)

High-resolution melting (HRM) analysis was performed in a CFX96 Real-Time PCR Detection System (Bio-Rad), equipped with HRM capability. Reactions were prepared in a final volume of 10 µL, containing 5 µL of master mix with saturating intercalating dye (SsoFast™ Evagreen® Supermix Bio-Rad), 0.5 µL of each primer (10 µM), 3 µL of nuclease-free ultrapure water, and 1 µL of template DNA (10 ng/µL).

The amplification protocol consisted of an initial denaturation at 95 °C for 3 minutes, followed by 40 cycles of denaturation at 95 °C for 10 seconds, annealing for 30 seconds, and extension at 72 °C for 20 seconds. Importantly, the annealing temperature was not fixed, but rather optimized according to each primer pair used. Multiple primer combinations were tested for both *R. rosea* and *E. senticosus*, and annealing temperatures ranged from 58 °C to 65 °C. These variations aimed to maximize the specificity and resolution of melting profiles. As detailed in Table 7 and 8, primers targeting *R. rosea* were tested predominantly at annealing temperatures between 58 °C and 60 °C, while those designed for *E. senticosus* were evaluated at temperatures between 62 °C and 65 °C.

HRM analysis was conducted by increasing the temperature from the annealing point to 95 °C in increments of 0.2 °C every 5 seconds, with continuous fluorescence acquisition. Fluorescence data were collected using Bio-Rad CFX Maestro 1.1, and melting curve analysis was performed with the Precision Melt Analysis Software 1.3 (Bio-Rad Laboratories, Hercules, CA, USA). Melting profiles were interpreted based on both curve shape and melting temperature (Tm), enabling discrimination between authentic samples and potential adulterants. Cluster analysis was carried out using the software's default parameters, with a curve shape sensitivity of 50% and a minimum Tm difference threshold of 0.15 °C.

4. RESULTS AND DISCUSSION

Plant material was oven-dried, mechanically disrupted and ground to a fine powder using a Precelys® homogenizer, ensuring efficient cell lysis and improved DNA release.

High-quality genomic DNA is essential for reliable downstream molecular analyses, including PCR, qPCR and HRM. Both *Rhodiola spp*. and *Eleutherococcus spp*. are chemically complex matrices, rich in polysaccharides, phenolic compounds, and triterpenoid saponins, which are known to inhibit DNA polymerase and compromise amplification efficiency (Porebski et al., 1997; Jobes et al., 1995; Schrader et al., 2012). Moreover, polyphenols can oxidize to quinones that covalently bind DNA, leading to reduced yield and browning of extracts (Wilkins and Smart, 1996), whereas polysaccharides increase viscosity, compromise DNA–silica interactions and reduce A260/230 purity ratios (Varma et al., 2007). Although CTAB-based protocols are frequently applied for polyphenol-rich matrices (Doyle and Doyle, 1990), silica-membrane kits offer greater reproducibility, safer handling and compatibility with large sample sets. In this work, genomic DNA was extracted using the NucleoSpin® Plant II Kit (Macherey-Nagel), which efficiently binds nucleic acids under chaotropic conditions. To minimise co-extraction of polyphenols and polysaccharides from leaves, roots and stems of *Rhodiola spp*. and *Eleuterococcus spp.*, an additional PW2 wash step was incorporated, improving membrane cleaning and downstream purity.

DNA concentration and purity were evaluated in triplicate using a SPECTROstar Nano spectrophotometer (BMG Labtech, Germany). Most samples evidenced A260/A280 ratios between 1.6 and 2.0, close or within values considered suitable for downstream analyses. Nevertheless, there were some exceptions, with five samples showing values between 0.7 and 1.3, and sample R11 reaching the lowest value of 0.4. The extracts were subsequently normalized to 10 ng/µL prior to PCR and real-time PCR coupled with HRM to ensure comparability of amplification efficiency across samples with different origins and matrices (Costa et al., 2015; Grazina et al., 2023).

4.1 *Rhodiola* spp.

4.1.1 *DNA Extraction and Quantification*

A total of 36 *Rhodiola* samples, including *R. rosea* and related taxa such as *R. kirilowii, R. crenulata, R. heterodonta, R. yunnanensis, R. porterbaw, R. bupleuroides, R. stephanii, and*

R. pachyclados, were analyzed. These samples included realistic matrices relevant to botanical authentication as whole plant tissue from botanical gardens, as well as commercial dried roots and powders.

DNA recovery was generally successful. Measured concentrations ranged from ~1 ng/µL (R6, *R. heterodonta*) to >100 ng/µL in commercial *R. rosea* root material (R31, R32). Most extracts showed good purity values as the ratio A280/A260 ranged from 1.8-2.0. In most samples, PCR with universal plant barcoding primers (ITS2 and rbcL) produced a single, distinct band of the expected size, indicating that the modified NucleoSpin® Plant II protocol with an additional PW2 wash yields amplifiable DNA even from processed herbal products.

Amplification failure occurred in specific cases (R12, R10, R6, R36) and was consistently associated with sample quality rather than with primer performance, namely:

- Severe fungal contamination/degradation

  R12 (*R. rosea*, visibly fungus-contaminated plant material) produced no measurable DNA and did not amplify. This suggests biological deterioration of the original tissue and microbial overgrowth, rather than a technical extraction failure.
- Extremely low plant DNA recovery/severe degradation

  R10 (*R. porterbaw*) and R15 (*R. rosea*, Coimbra) were old samples from herbarium and showed very low DNA yields and did not amplify.

  R6 (*R. heterodonta*) yielded ~1 ng/µL and produced only a very faint band, indicating that template availability was near the lower functional limit for reliable PCR.
- Inhibitor carryover / degraded template despite measurable yield

  R36 (*R. rosea*, whole plant from Bergius Botanic Garden) produced measurable DNA (~29 ng/µL) but did not amplify. Since other botanical garden samples amplified under identical conditions, this suggests the presence of inhibitors or specific degradation of this sample.

In contrast, purified DNA extracted from reference samples provided by the Kew Royal Botanic Gardens (R27–R29), consistently produced amplicons with the expected size.

Overall, most *Rhodiola* samples, including commercial powders and marketed roots, showed to have amplifiable DNA and produced clean, single-band amplification (Table 11).

Table 11 – DNA concentration and amplification results for *Rhodiola*.

Sample ID	Species	Sample type	DNA concentration (ng/µL)	Purity (A260/A280	Amplification result
R1	*R. rosea*	Root	24.2	1.5	+
R2	*R. rosea*	Powder	12.2	1.0	+
R3	*R. rosea*	Seed	—	—	–
R4	*R. rosea*	Whole plant	36.3	1.7	+
R5	*R. kirilowii*	Whole plant	29.9	1.8	+
R6	*R. heterodonta*	Whole plant	1.1	0.7	+
R7	*R. rosea*	Powder	47.9	0.9	+
R8	*R. rosea*	Tablet	—	—	–
R9	*R. rosea*	Whole plant	13.2	1.3	+
R10	*R. porterbaw*	Whole plant	1.2	0.9	–
R11	*R. crenulata*	Whole plant	13.4	0.4	+
R12	*R. rosea*	Fungal-contaminated plant	—	—	–
R13	*R. rosea*	Whole plant	16.9	1.6	+
R14	*Rhodiola* sp.	Whole plant	60.5	1.6	+
R15	*R. rosea*	Whole plant	2.3	1.2	–
R16	*R. bupleuroides*	Whole plant	19.5	1.9	+
R17	*R. heterodonta*	Whole plant	15.6	1.8	+
R18	*R. stephanii*	Whole plant	19.1	1.8	+
R19	*R. kirilowii*	Whole plant	26.9	1.8	+
R20	*R. yunnanensis*	Whole plant	13.8	1.7	+
R21	*R. rosea*	Whole plant	46.3	1.5	+
R22	*R. pachyclados*	Whole plant	17.4	1.9	+
R23	*R. kirilowii*	Whole plant	26.5	1.7	+
R24	*Rhodiola* sp.	Whole plant	48.6	1.8	+
R25	*R. rosea*	Whole plant	59.6	1.8	+
R26	*R. rosea*	Whole plant	8.2	1.9	+
R27	*R. crenulata*	Purified DNA	~50 ng/µL	2.0	+
R28	*R. crenulata*	Purified DNA	~50 ng/µL	2.0	+
R29	*R. yunnanensis*	Purified DNA	~50 ng/µL	2.0	+
R30	*R. rosea*	Root	44.6	1.9	+
R31	*R. rosea*	Root	107.4	2.1	+
R32	*R. rosea*	Root	105.3	2.0	+
R33	*R. rosea*	Root	27.7	2.0	+
R34	*R. rosea*	Powder	62.6	2.0	+
R35	*R. rosea*	Root	56.2	1.9	+
R36	*R. rosea*	Whole plant	29.4	1.6	–

Concentrations represent mean values of triplicate readings; "—" indicates undetectable DNA concentration. Samples R28–R30 correspond to purified DNA extracts supplied by the Royal Botanic Gardens, Kew.

4.1.2 *PCR Amplification - Rhodiola rosea*

After DNA extraction, all extracts were initially evaluated for the integrity and amplifiability of the genetic material to ensure that only suitable extracts were carried forward to the subsequent steps of specific PCR and HRM. As described in the methodology, the first screening was performed using the universal ITS2 barcode, amplified with primers ITS-S2F and ITS-S4R, which generate a fragment with a typical length between ~380–420 bp.

Gel analysis (Figure 4) showed that most samples presented a single, well-defined band of the expected size, indicating the presence of DNA suitable for amplification. However, five samples did not show any visible product, suggesting possible DNA degradation or the presence of co-extracted inhibitors.

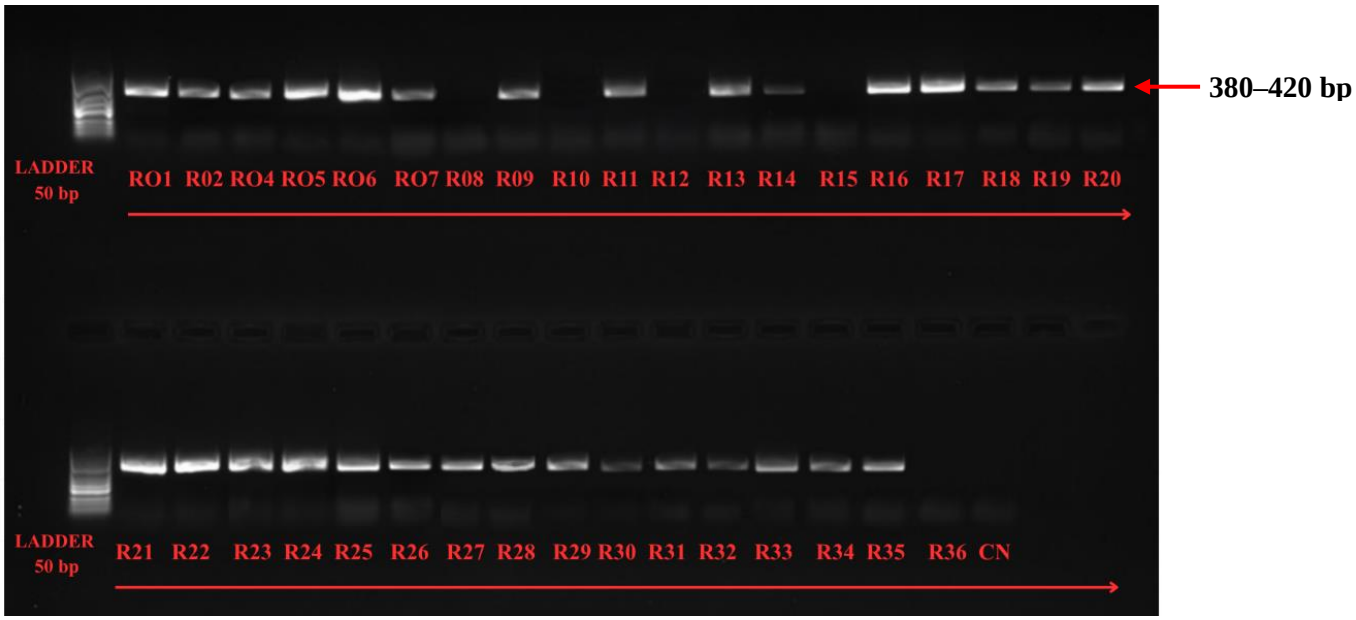

Figure 4: Result of *Rhodiola* spp. samples amplification using ITS-S2F/ ITS-S4R (~380–420 bp).

To verify whether the observed non-amplifications were specifically related to the ITS2 target or reflected low quality of the extract/high degradation of DNA, the samples were re-evaluated using a second universal marker widely employed in plants: the chloroplast gene rbcLa, amplified with primers rbcLa-F and rbcLa-R, which generate a fragment of approximately 550–600 bp. As shown in Figure 5, these samples again failed to amplify. The non-amplification with two robust universal markers suggests that the DNA in these five samples was excessively degraded or the extract contained significant levels of inhibitors incompatible with the PCR reaction.

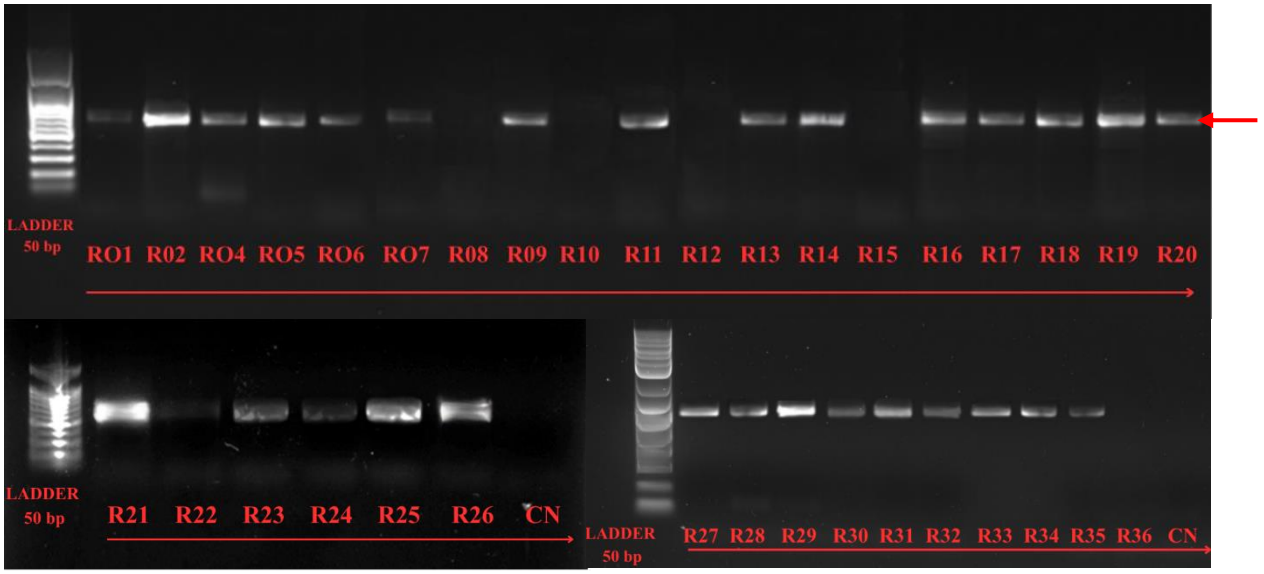

Figure 5: Result of *Rhodiola* spp. samples amplification using rbcLa-F/ rbcLa-R

Given the inability to obtain consistent amplification, samples R08, R10, R12, R15 and R36 were considered unsuitable to proceed with the molecular analysis, and were therefore discarded.

4.1.3 Species-Specific PCR

To select the most suitable species-specific primer system for *R. rosea* authentication and to identify candidates potentially compatible with downstream HRM analysis, three primer pairs (RodR3-F/RodR2-R, RodR2-F/RodR2-R, and Rd-HRM2-F/Rd-HRM2-R) were initially evaluated (Table 8). As a first step, PCR optimization using a temperature-gradient assay was performed to determine the best annealing conditions.

Figure 6 shows the amplification results obtained for the two primer pairs designed to specifically target *R. rosea* DNA tested under low and higher stringency annealing conditions. The primer pair RodR2-F/RodR2-R, tested at 50 °C and 52 °C, produced a faint but discernible band exclusively in the reference sample P72 (R02). No amplification was observed for Brazilian ginseng (P35), nor for mixtures of DNA from other plant species, suggesting primer specificity.

In contrast, the RodR3-F/RodR2-R primer pair, tested at 48 °C and 50 °C, generated non-specific amplification in sample P35 and mixture ML2 at 48 °C, and P35 at 50 °C. At higher annealing temperatures, no nonspecific amplification bands were observed. Nevertheless, the generally weak band intensity suggests a reduced reaction efficiency.

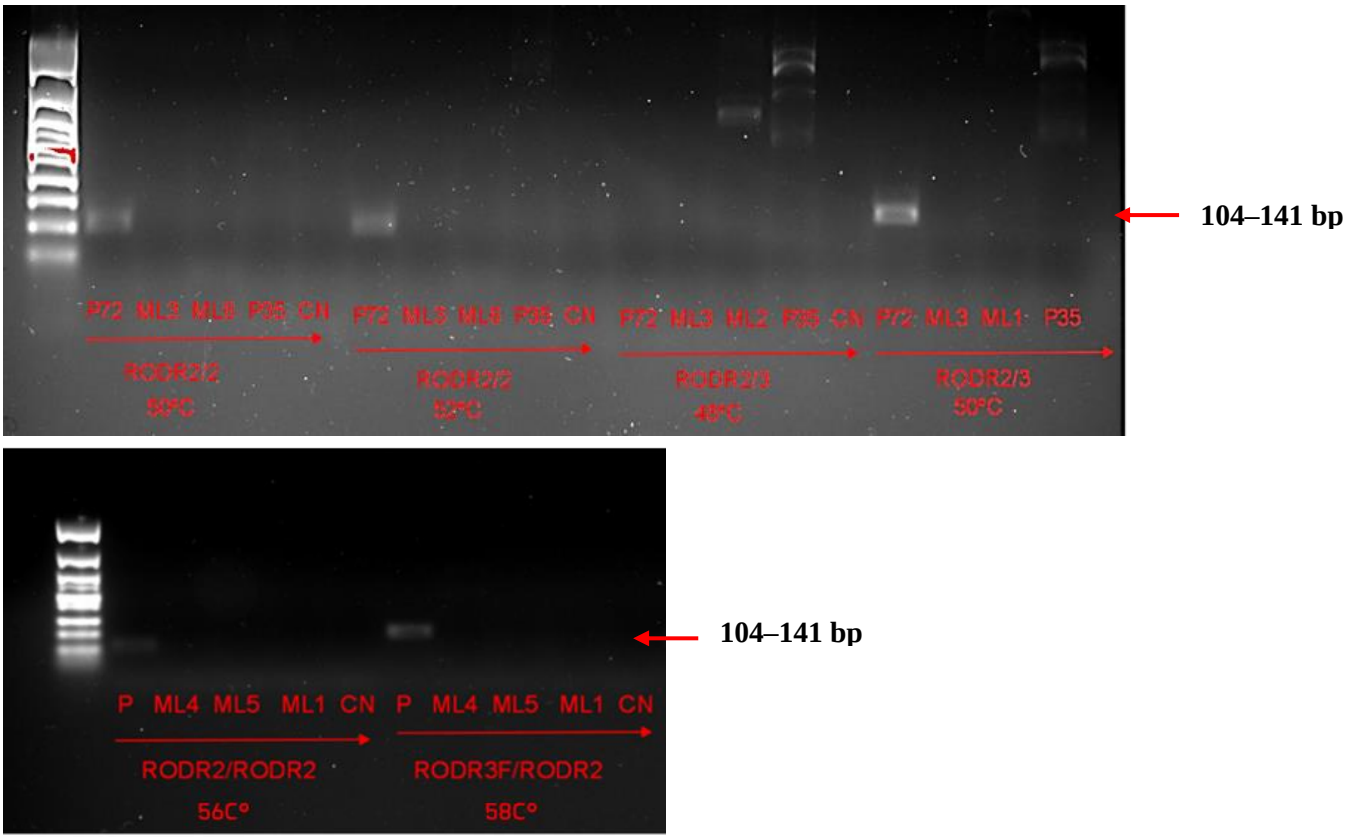

Figure 6 – Results of PCR amplification using primers RodR2-F/RodR2-R and RodR2-F/RodR3-R at different annealing temperatures

Figure 7 presents the results obtained for primers Rd-HRM1-F/Rd-HRM1-R1, which were designed to bind to different species of the Rhodiola genus in a sequence containing different SNPs, aiming for species discrimination based on HRM. At an annealing temperature of 56 ºC, the positive control (*R. rosea*) showed a positive amplification; however, cross-reactivity was observed with the DNA mixture ML4 and, to a lesser extent, ML1. Trying to overpass the problem of low specificity under the tested conditions, the annealing temperature was increased to 58 ºC. In this case, no cross-reactivity was observed, however also no amplification was obtained with this primer set. Therefore, this primer set was discarded, and further assays were carried out with the second primer set designed for HRM purposes, Rd-HRM2-F/Rd-HRM2-R.

Figure 7 – Results of PCR amplification using primers Rd-HRM1-F/Rd-HMR1-R under different annealing temperatures

After establishing the best annealing temperatures, a series of mixtures containing DNA (10ng/µL) of different plant species traditionally used for brain health (ML1-ML10, see annex A for the detailed list of species) and DNA extracts obtained from commercial mixtures of plant, were used to test cross-reactivity of the selected conditions against a broader range of species.

Figure 8 shows the amplification results using the primer pair RodR2-F/RodR3-R at an annealing temperature of 58 °C, which evidences a positive amplification for the positive control. In contrast, the mixtures showed an absence of the expected band, demonstrating the specificity of the primers.

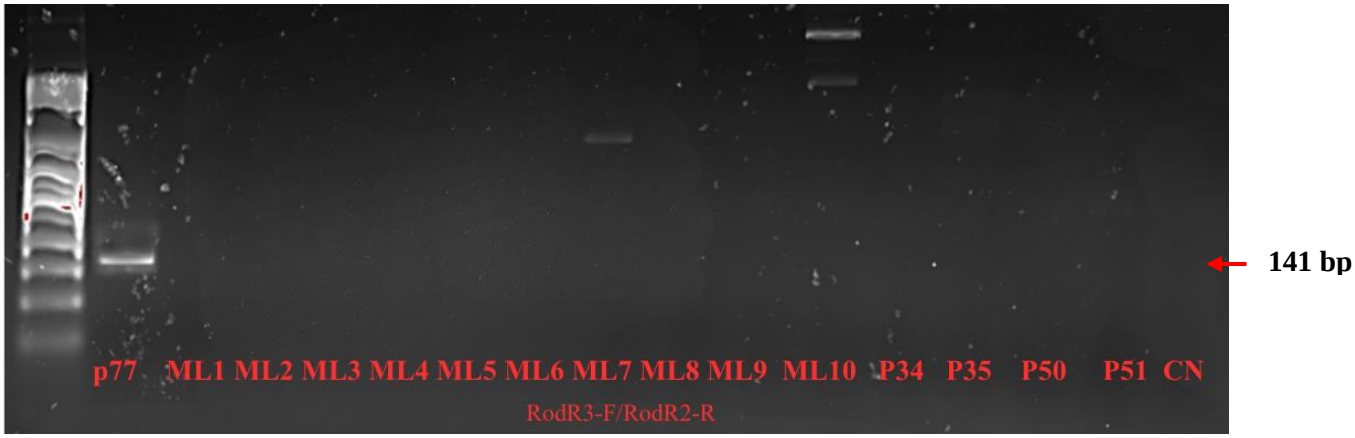

Figure 8 – Results of PCR amplification using RodR3-F/RodR2-R (annealing at 58 °C)

Similarly, the cross-reactivity of primer set RodR2-F/RodR2-R was also evaluated against the same mixtures (Figure 9), which also evidenced the absence of cross-amplification with DNA from other plant species used for similar therapeutic purposes as those of *R. rosea*. A non-specific amplification was observed against ML7 and ML10, however, corresponding to bands of high length.

Figure 9 – Results of PCR amplification using RodR2-F/RodR2-R (annealing at 56 °C)

Finally, the primer set Rd-HRM2-F/Rd-HRM2-R was also tested for cross-reactivity purposes, using the same mixtures of DNA and commercial products containing several different medicinal plants (Figure 10). Once again, DNA from some plant species generated unspecific amplification bands, however, all showed the absence of the expected band with 116 bp length.

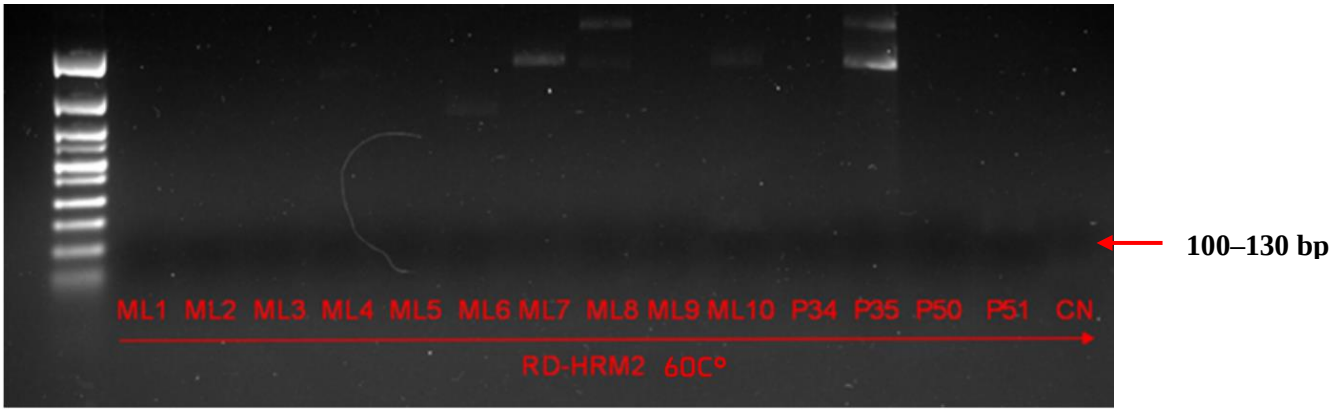

Figure 10 - Results of PCR amplification of Rhodiola extracts using RD-HRM2-F/RD-HRM2-R (annealing at 60 °C)

Subsequently, the three primer sets that demonstrated acceptable specificity in the cross-reactivity assays, were tested by using real-time PCR coupled with High-Resolution Melting (HRM) analysis. This methodology, already established as highly sensitive for detecting minimal sequence variation, represents a key approach for the authentication of species within the genus *Rhodiola*, hopefully enabling discrimination of melting profiles among different *Rhodiola* species. Furthermore, HRM allows simultaneous assessment of specificity, reproducibility, and intra- and interspecific variability without the need for post-PCR steps, thereby reducing contamination risks and increasing analytical rigor.

4.1.4 Real-time PCR coupled with HRM analysis

Primer set Rd-HRM2-F/Rd-HRM2-R

The amplification reactions performed with the Rd-HRM2-F/R primer pair showed well-defined and reproducible amplification curves across all tested samples. All *R. rosea* samples were highlighted in blue to facilitate visual comparison, allowing clear assessment of their intra-specific behaviour.

Sample P77 (*R04, R. rosea*), displayed in blue in Figure 11, showed the most efficient amplification (Cq = 15.05), indicating strong primer–target affinity. Other *R. rosea* samples also amplified efficiently, with Cq values ranging from 13.84 to 18.22, although their curves exhibited noticeable differences in slope and intensity. Non-target *Rhodiola* species exhibited higher Cq values (up to 35.83), which may be attributed to reduced primer binding affinity due to potential mismatches. The negative control did not amplify, confirming the absence of contamination.

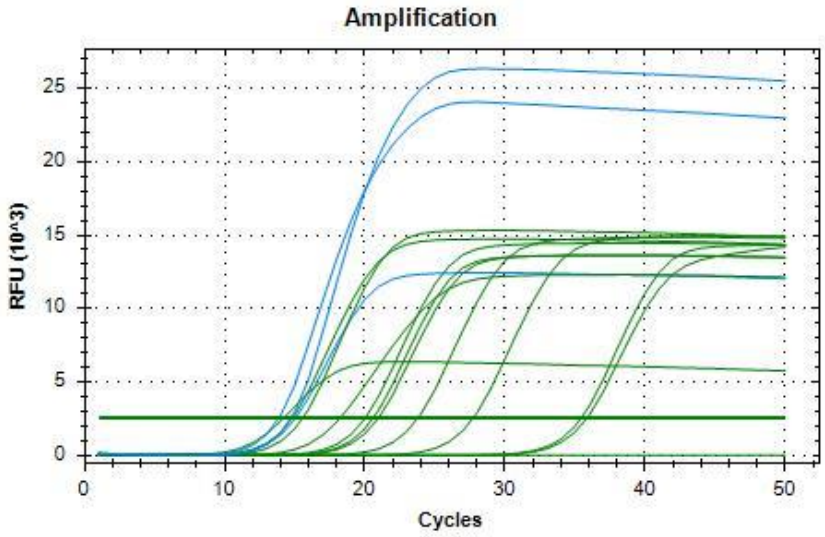

Figure 11 - Real-time PCR amplification curves obtained with the Rd-HRM2-F/R primer. Blue curves represent Rhodiola rosea *samples, while green curves correspond to non-target species. The negative control showed no amplification.*

The melt curves (Figure 12, left) generated with the Rd-HRM2-F/R primer set exhibited a single melting transition for all samples, confirming the amplification of a unique and specific PCR product. However, the *R. rosea* samples tested (highlighted in blue) displayed slightly distinct melting among themselves, with subtle but consistent shifts in curve shape and decay temperature, suggesting possible intra-specific sequence variation within *R. rosea*.

The melt peak (Figure 12, right) plot further highlights the differences observed between *R. rosea* samples and among other species of *Rhodiola* genus.

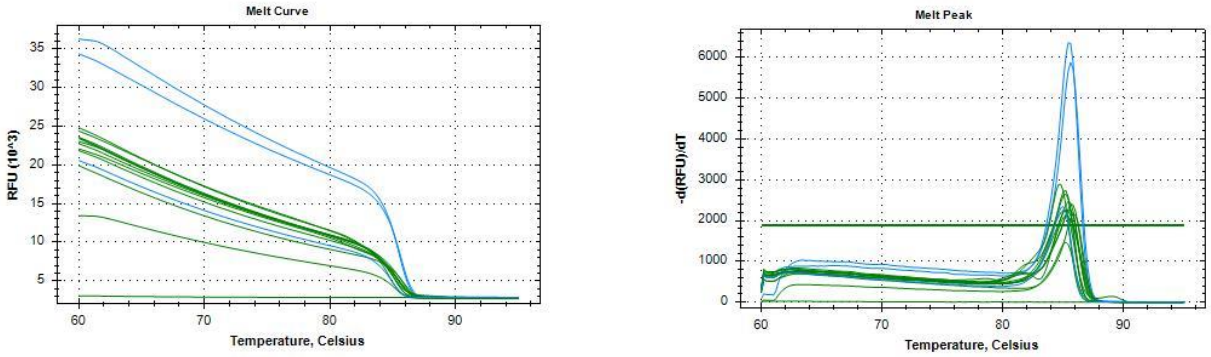

Figure 12 – Conventional melt curves (left) and melting peak (right) obtained by real-time PCR amplification with EvaGreen dye (*Rhodiola rosea* in blue and non-target *Rhodiola* species in green).

Following real-time PCR amplification, the obtained amplicons were subjected to HRM analysis to evaluate the discriminatory capacity of the Rd-HRM2-F/R primer set. The HRM approach allowed a detailed assessment of melting-profile variation among *R. rosea* and closely related *Rhodiola* species.

The normalized melt curves (Figure 13) revealed that the tested samples did not form a single homogeneous melting cluster. Instead, three clearly distinguishable melting patterns emerged, indicating the presence of three major HRM clusters. The profiles differed in the shape and position of the melting transitions, demonstrating sequence variability among samples within the *Rhodiola* complex.

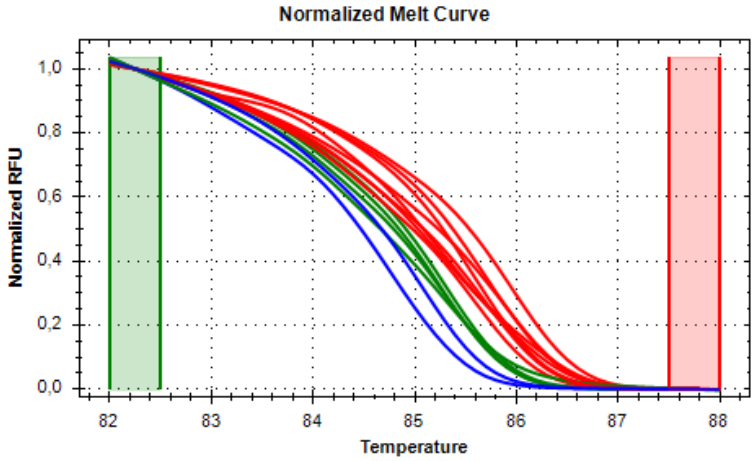

Figure 13 – Normalized melt curves obtained by real-time PCR amplification with EvaGreen dye *for Rhodiola samples using the Rd-HRM2-F/R primer set*

To enhance the visualization of these differences, the data were plotted as difference curves (Figure 14). This representation amplified the separation between melting signatures and

allowed clear definition of cluster boundaries.

Samples assigned to Cluster 1 showed a characteristic melting behaviour with higher fluorescence retention over the melting interval, whereas Cluster 2 displayed an intermediate profile marked by a slight leftward shift. Cluster 3, in contrast, represented the most divergent group, exhibiting a pronounced downward melt-transition displacement, consistent with a distinct sequence polymorphism relative to the other clusters. The HRM software assigned samples to three distinct clusters with high degree of confidence (≥ 96%), as summarized in Table 12. The distribution of *R. rosea* across more than one cluster indicates that, although Rd-HRM2-F/R enables some differentiation between species, it also captures natural genetic variation within *R. rosea*. Since one sample of *R. rosea* accessions was grouped into Cluster 3, this may suggest intra-specific polymorphism within *R. rosea* for this locus. Importantly, the HRM software classified several non-target *Rhodiola* species (e.g., *R. crenulata, R. heterodonta, R. stephanii, R. kirilowii*) into Cluster 1 together with two samples of *R. rosea*. Similarly, the three samples of R. *kirilowii* also showed a high variability since they were dispersed among the three clusters, evidencing either a high variability of the ITS region in this genus, or possibly, a misidentification of the voucher plants.

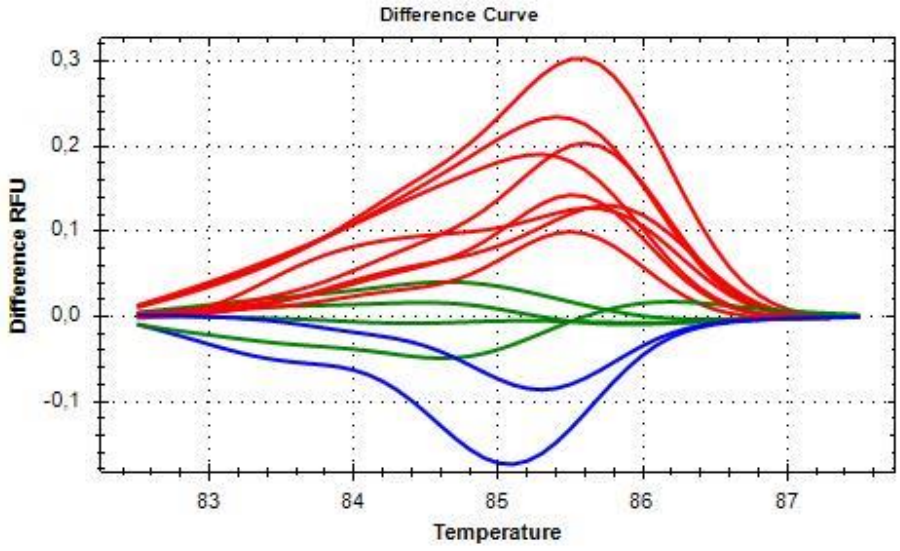

Figure 14 – Difference curve plot obtained by real-time PCR amplification with EvaGreen dye *showing HRM cluster separation among Rhodiola samples using the Rd-HRM2-F/R primer.*

Table 12 – HRM cluster assignment for *Rhodiola* spp. samples analyzed with Rd-HRM2-F/R primer set.

Sample Code	Species	Cluster	Confidence (%)	Ref
R17	*R. heterodonta*	Cluster 1	96.6	
R6	*R. heterodonta*	Cluster 1	96.1	
R8	*R. rosea*	Cluster 1	96.0	
R11	*R. crenulata*	Cluster 1	98.0	
R18	*R. stephanii*	Cluster 1	97.6	
R19	*R. kirilowii*	Cluster 1	96.3	
R21	*R. rosea*	Cluster 1	97.1	
R25	*R. rosea*	Cluster 1	97.1	
R5	*R. kirilowii*	Cluster 2	96.5	
R20	*Rhodiola* sp.	Cluster 2	96.5	
R24	*Rhodiola* sp.	Cluster 2	96.5	
R4	*R. rosea*	Cluster 3	96.9	
R23	*R. kirilowii*	Cluster 3	96.7	

Real-time PCR and HRM with Primer set RodR3-F/RodR2-R

The amplification reactions performed with the RodR3-F/RodR2-R primer pair revealed marked differences in amplification efficiency between *R. rosea* and non-target *Rhodiola* species. As shown in Figure 15, only the reference sample P77 (R04- *R. rosea*) displayed efficient amplification (Cq = 14.13), confirming strong affinity of this primer set for the target species. A second *R. rosea* sample (P72 – R02) also amplified, although with a later Cq (~22.8), despite all samples being normalized to an initial concentration of 10 ng/µL.

Several non-target *Rhodiola* species, including *R. kirilowii* (R5), *R. heterodonta* (R6), *R. crenulata* (R12), and *R. kirilowii* (R14), also produced amplification curves, though with variable Cq values (12.91–33.27). Although this primer set was initially designed aiming for a high specificity against *R. rosea*, which was demonstrated in the *in silico* analysis, the obtained results indicate cross-reactivity of the RodR3-F/RodR2-R primer with multiple *Rhodiola* species, revealing limited discriminatory power when applied to complex matrices.

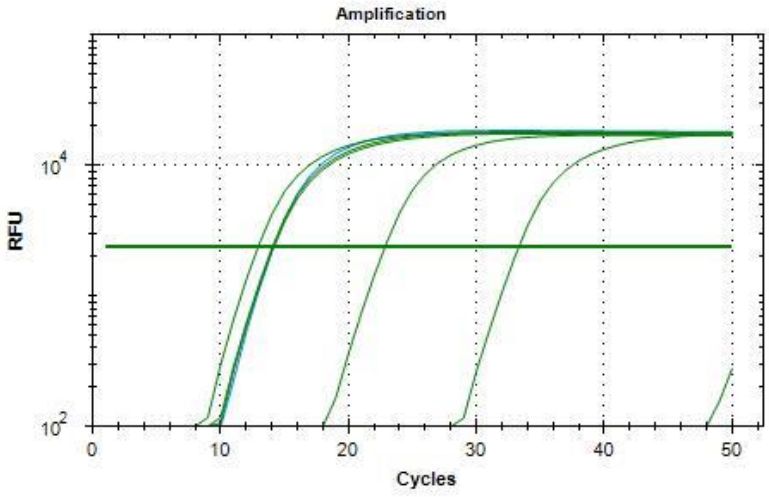

Figure 15 – Real-time PCR amplification curves using EvaGreen dye obtained using the RodR3-F/RodR2-R primer.

The melt curve and melt peak analysis (Figure 16) revealed a single melting domain for all amplified samples, confirming that RodR3-F/RodR2-R generated a single amplicon across both target and non-target taxa. Although *R. rosea* samples showed peaks around 87–88 °C, multiple non-target species displayed peaks within the same temperature range. The lack of clear separation between peak max confirms that RodR3-F/RodR2-R cannot distinguish *R. rosea* from other *Rhodiola* species based solely on melting temperature. However, despite showing similar Tm values, slight differences were observed among *Rhodiola* species.

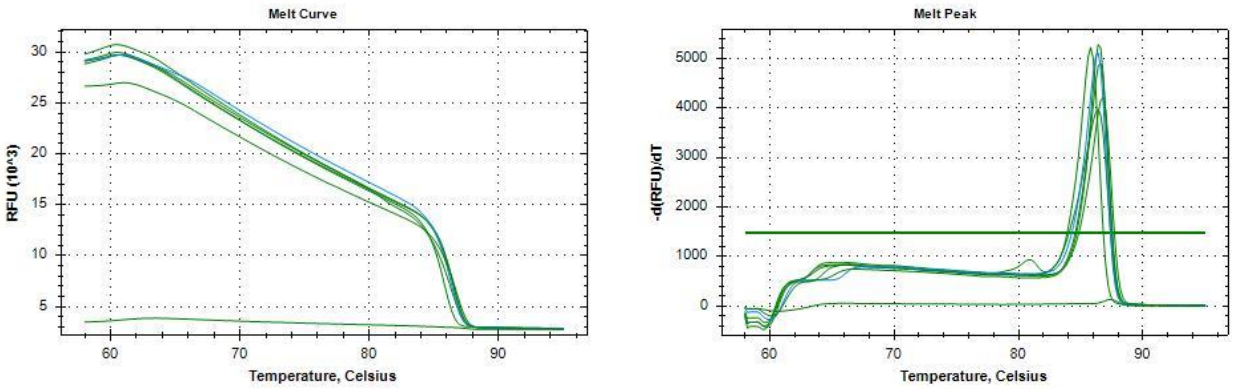

Figure 16 – Conventional melt curves (left) and melting peak (right) obtained by real-time PCR amplification with EvaGreen dye with RodR3-F/RodR2-R primer set.

Following the real-time PCR evaluation, all successfully amplified samples were subjected to High-Resolution Melting (HRM) analysis using the RodR3-F/RodR2-R primer pair.

The aim of this step was to assess the discriminatory capacity of this primer set and determine whether *R. rosea* samples formed a coherent cluster based on melting profile that could be reliably distinguished from other *Rhodiola* species.

The normalized melt curve (Figure 17A) revealed clear melting differences among the tested samples. Although all reactions produced a single amplicon, the melting transitions differed substantially in curve inflection, slope, and temperature shift. Notably, *R. rosea* samples did not group into a single melting profile. Instead, they separated into multiple melting domains, indicating the presence of intra-specific sequence variation within the amplified region. In contrast, different non-target species showed consistent melting signatures, forming visually distinct profiles relative to *R. rosea*.

The difference plot (Figure 17B) further enhanced the resolution of melting differences and confirmed the presence of six distinct cluster groups. These clusters corresponded to specific melting behaviors, each of a different *Rhodiola* taxa. Importantly, *R. rosea* samples were assigned into three distinct groups (Clusters 2, 3, and 6), indicating that the target region amplified by RodR3-F/RodR2-R exhibits significant intra-specific variability.

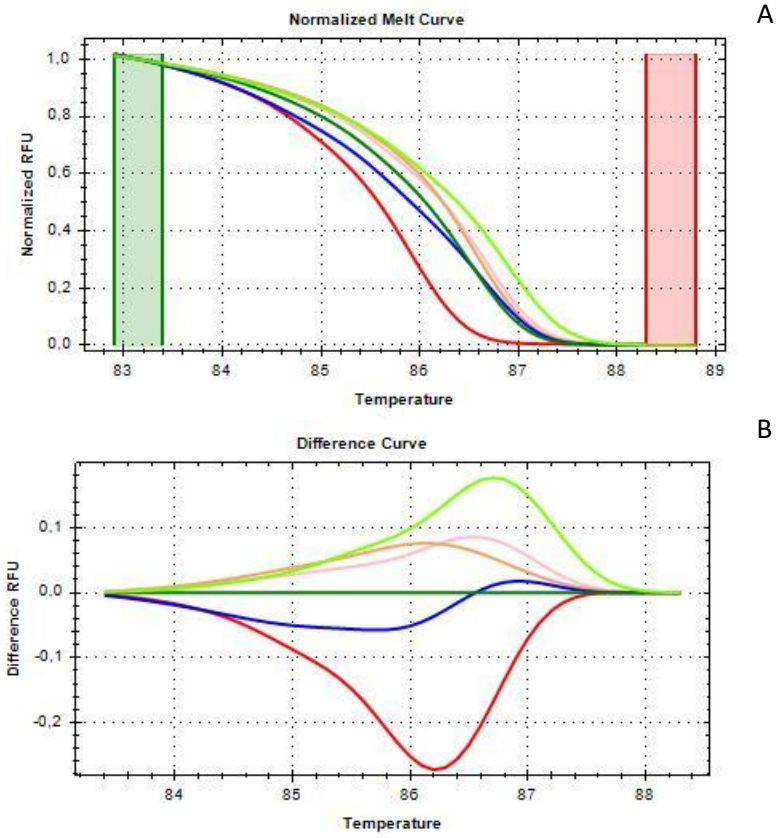

Figure 17A & 17 B– Normalized melt curves obtained using the RodR3-F/RodR2-R primer pair.

Instead of forming a single cohesive cluster, *R. rosea* samples appeared distributed across multiple groups, indicating detectable polymorphisms within the amplified region, as shown in Table 13. This pattern suggests the presence of intra-specific polymorphisms within *R. rosea* for the amplified region and highlights a reduced robustness of the assay for authentication purposes, as a single and consistent HRM signature is expected for reliable species identification.

Furthermore, the melting profiles of the non-target species formed well-defined and separate clusters, demonstrating high inter-specific resolution. However, the lack of clustering consistency among *R. rosea* samples indicates insufficient intra-specific uniformity, limiting the suitability of this marker for routine authentication workflows.

Table 13 – HRM cluster assignment for RodR3-F/RodR2-R primer set

Sample Code	Species	Cluster Assignment	% Confidence	Ref
R12	*Rhodiola rosea*	Cluster 1	86.6	
R4	*Rhodiola rosea*	Cluster 2	98.7	
R5	*Rhodiola kirilowii*	Cluster 3	100.0	
R6	*Rhodiola heterodonta*	Cluster 4	98.6	
R14	*Rhodiola* sp.	Cluster 5	89.1	
R1	*Rhodiola rosea*	Cluster 6	98.8	

Real-time PCR coupled with HRM using Primer set RodR2-F/RodR2-R

After the optimization step using conventional PCR, the RodR2-F/RodR2-R primer pair was selected for evaluation in real-time PCR followed by HRM analysis, in order to assess its performance in terms of amplification, specificity, and discriminatory capacity between *R. rosea* and non-target species. Experiments were conducted at two annealing temperatures (60 °C and 65 °C) to determine whether increasing stringency could improve the overall performance of the marker.

Testing using 60 °C as annealing temperature

The amplification curves obtained at 60 °C revealed inconsistent behavior among samples (Figure 19). Although some *R. rosea* samples specifically: R4, R12, and R14 exhibited efficient amplification (Cq between 13–14), other samples of the same species showed very high Cq values (above 30), indicating low primer–target affinity. Additionally, non-target species such as *R. kirilowii* (R5) and *R. heterodonta* (R6) also amplified with relatively low Cq values.

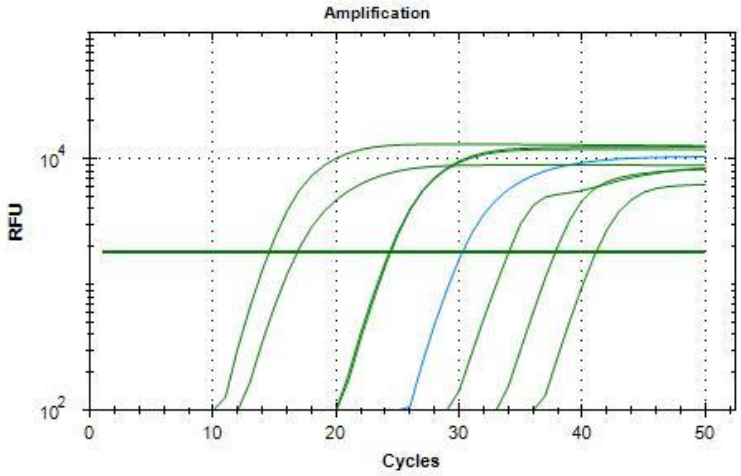

Figure 18 - Amplification curves obtained by real-time PCR using EvaGreen dye obtained with the RodR2-F/RodR2-R primer set using 60 ºC as annealing temperature.

The melting curves (Figure 20) showed unspecific amplification and possible primer-dimers. Therefore, the same experiment was repeated using more stringent conditions, with a higher annealing temperature.

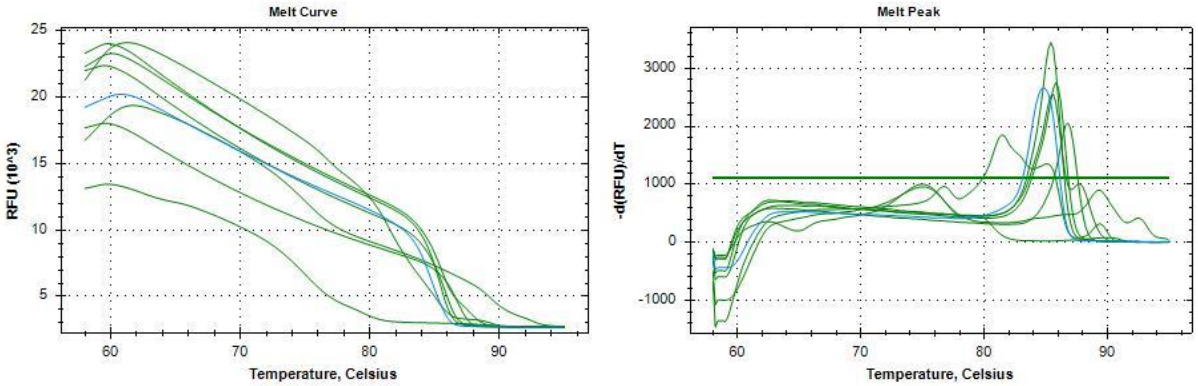

Figure 19 – Conventional melt curves (left) and melting peak (right) obtained by real-time PCR amplification with EvaGreen dye with RodR2-F/RodR2-R *primer set and annealing temperature of 60 ºC.*

Testing using 65 °C annealing temperature

With the increase in annealing temperature to 65 °C, a partial improvement in amplification consistency was observed (Figure 21), particularly for *R. rosea* samples (R1, R3, R4, R12, and R14), which showed Cq values between 13–24. Considering that this primer set was initially designed to specifically target *R. rosea*, undesired amplification of non-target species *R. kirilowii* (R5) and *R. heterodonta* (R6) persisted, demonstrating that increasing the

temperature was not sufficient to achieve acceptable specificity.

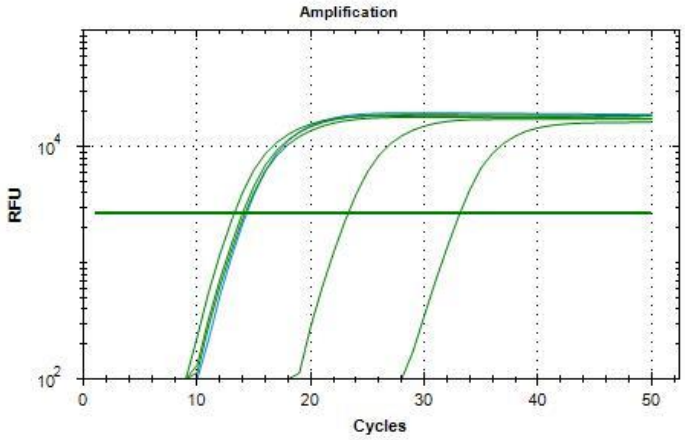

Figure 20 - Amplification curves obtained by real-time PCR using EvaGreen dye obtained with the RodR2-F/RodR2-R primer set using 65 ºC as annealing temperature

In the melting curves (Figure 22), the profiles were more uniform than at 60 °C, showing Tm intervals similar between different species and without the presence of unspecific amplicons and/or primer-dimers.

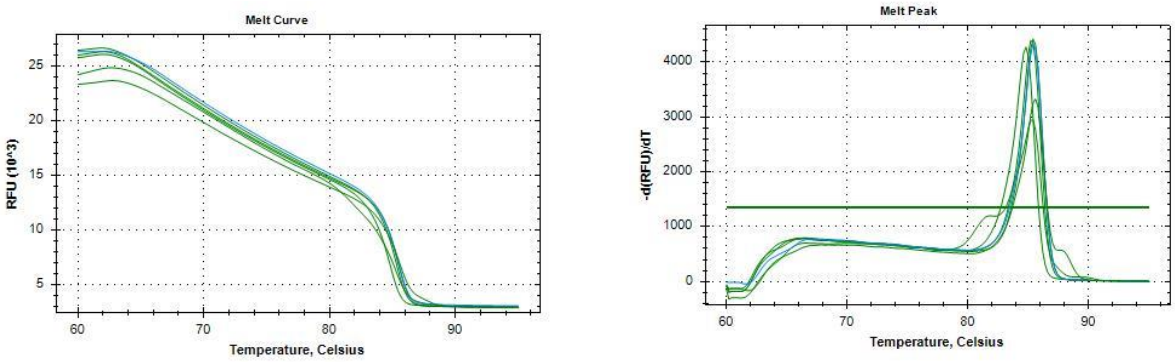

Figure 21 – Conventional melt curves (left) and melting peak (right) obtained by real-time PCR amplification with EvaGreen dye with RodR2-F/RodR2-R primer set and annealing temperature of 60 ºC.

Different clusters were evident in the normalized melt curves (Figure 22), indicating that three distinct samples of *R. rosea* clustered into three separate groups (Table 14). Cluster analysis showed that *R. rosea* (R4) was grouped together with the sample of *Rhodiola sp*. (R38) in Cluster 1, while *R. rosea* accessions R1, R12 were placed in independent clusters (Clusters 2 and 5). *R. heterodonta* (R6) and *R. kirilowii* (R5) formed Clusters 3 and 4, respectively. Once again, *R. rosea* did not form a single coherent cluster.

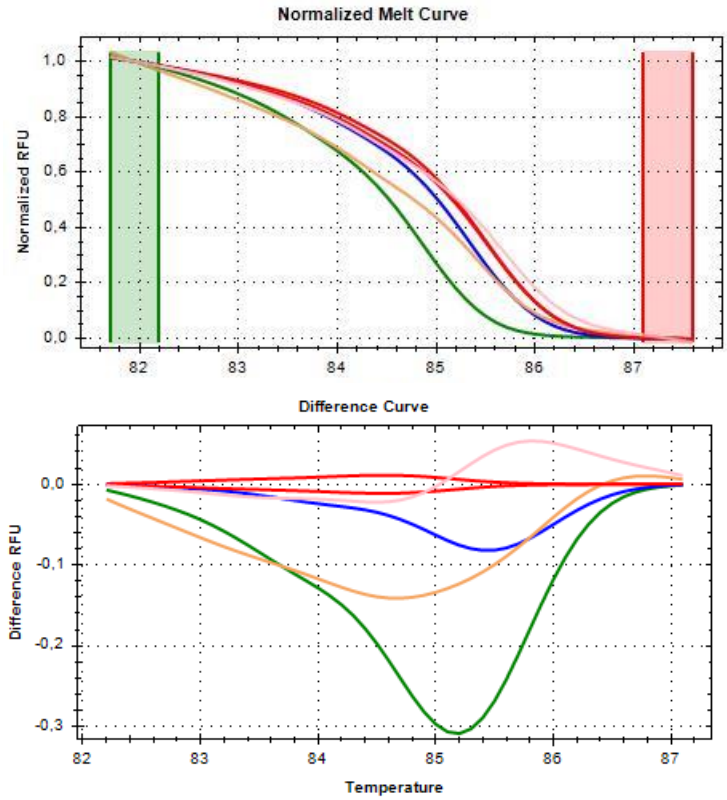

Figure 22 – Normalized melt curves obtained by real-time PCR with EvaGreen dye using RodR2-F/RodR2-R primer set (annealing at 65 °C).

Table 14 – HRM cluster assignment for Rhodiola samples analysed with RodR2-F/RodR2-R at 65 °C

Sample code	Species	Cluster	% Confidence	Ref
R4	*R. rosea*	1	99.8	
R14	*Rhodiola* sp.	1	99.7	
R12	*R. rosea*	2	99.8	
R6	*R. heterodonta*	3	99.7	
R5	*R. kirilowii*	4	100.0	
R1	*R. rosea*	5	97.4	

Taken together, the HRM results using either of the three primer sets tested showed that they are not suitable as a diagnostic primer pair for authenticating *R. rosea*. Different samples of this species were distributed across multiple clusters, demonstrating either intra-specific variability or misidentification in the voucher samples.

4.2 Eleutherococcus spp.

4.2.1 DNA Extraction and Quantification

Genomic DNA was successfully extracted from all *Eleutherococcus* samples, which included fresh/whole plant tissues, root material, and commercial powders of *E. senticosus*. Despite the high lignification and high triterpenoid saponin content typically reported for this genus, the modified extraction protocol proved to be effective.

DNA concentrations ranged from 7.3 ng/µL (*E. leucorrhizus*, E1) to 167.0 ng/µL (*E. senticosus*, E16). With some exceptions, purity was generally good, as the ratio A260/A280 was predominantly 1.7 or 1.8. Nevertheless, some samples showed lower values, with the lowest (0.8) corresponding to sample C4. Importantly, all *Eleutherococcus* extracts produced clear, single bands with universal barcoding primers (rbcL and ITS2), confirming that the recovered DNA was not only quantifiable but also amplifiable across different matrix types, including commercial powders.

These results indicate that the modified NucleoSpin® Plant II protocol with the additional PW2 wash proved robust for *Eleutherococcus spp*. DNa extraction, providing DNA with sufficient quality for downstream species-specific assays and HRM profiling (Table 15).

Table 15 – DNA concentration measured by spectrophotometry and amplification results for *Eleutherococcus* spp. samples.

Sample ID	Species	Sample type	DNA concentration (ng/µL)	Purity (A260/A280	Amplification Result*
E1	*E. leucorrhizus*	Whole plant	7.3	1.2	+
E2	*E. lasiogyne*	Whole plant	8.7	1.4	+
E3	*E. lasiogyne*	Whole plant	11.3	1.5	+
E4	*E. lasiogyne*	Whole plant	8.7	0.8	+
E5	*E. henryi*	Whole plant	27.6	1.8	+
E6	*E. senticosus*	Whole plant	39.1	1.8	+
E7	*E. leucorrhizus*	Whole plant	12.2	1.5	+
E8	*E. leucorrhizus*	Whole plant	19.2	1.7	+
E9	*E. leucorrhizus*	Whole plant	16.6	1.7	+
E10	*E. leucorrhizus*	Whole plant	18.5	1.8	+
E11	*E. divaricatus*	Whole plant	29.0	1.3	+
E12	*E. henryi*	Whole plant	22.3	1.7	+
E13	*E. senticosus*	Root	29.0	1.2	+
E14	*E. senticosus*	Root	167.0	1.7	+
E15	*E. senticosus*	Powder	15.4	1.1	+

E16	*E. senticosus*	Root	31.6	1.7	+
E17	*E. senticosus*	Root	22.4	1.6	+
E18	*E. senticosus*	Root	11.7	1.4	+
E19	*E. senticosus*	Powder	18.7	1.2	+
P32	*E. senticosus*	Whole plant	22.9	1.8	+
P54	*Pfaffia glomerata*	Whole plant	28.7	1.7	+
P59	*E. senticosus*	Whole plant	22.3	1.8	+
P124	*E. senticosus*	Powder	29.0	1.1	+

* PCR using ITS-S2F/ ITS-S4R and rbcLa-F/ rbcLa-R primers.

4.2.2 PCR Amplification - *Eleutherococcus senticosus*

For *Eleutherococcus* samples, amplifiability was first assessed using primers rbcLa-F/rbcLa-R. As presented in Figure 23, all *Eleutherococcus* extracts amplified successfully following DNA extraction, producing clear single amplicons at the expected size, confirming adequate DNA integrity and absence of inhibitory compounds. Since all samples generated an expected fragment with size of ~550–600 bp, PCR amplification with ITS2 primers was not performed.

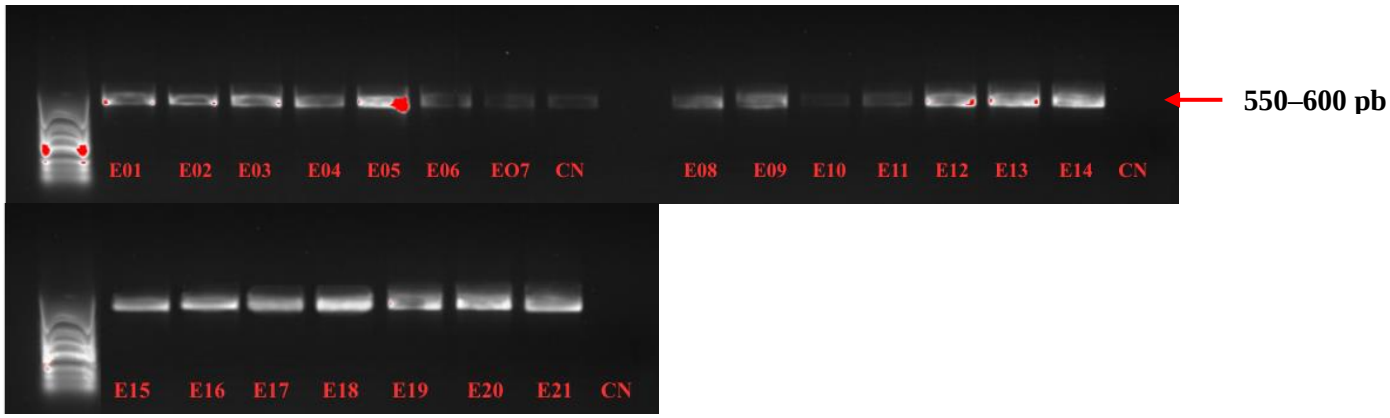

Figure 23: Results of PCR amplification of *Eleutherococcus* extracts using rbcLa-F/rbcLa-R (~550–600 bp).

To evaluate amplification efficiency and target specificity, all species-specific primer pairs designed for *E. senticosus* were screened under standardized PCR conditions at an annealing temperature of 60 °C. Assays were performed using authenticated *E. senticosus* (P124), four *Eleutherococcus* species (E1–*E. leucorrhizus*, E2–*E. lasiogyne*, E5–*E. henryi*, E11–*E. divaricatus*) and the non-target control *Pfaffia glomerata* (P54).

As shown in Figures 24 and 25, the primer sets Esent1-F/Esent1-R and EsentFDS-

F/EsentFDS-R produced clear, single amplicons for *E. senticosus* (P124) and for all *Eleutherococcus* species tested, with no amplification detected for the non-target sample P54. Both primer pairs displayed an identical specificity profile, demonstrating reliable discrimination of *Eleutherococcus* DNA and absence of cross-reactivity with *P. glomerata*.

In contrast, the primer sets EsentBAS2-F/EsentBAS2-R and EsentCYP-F/EsentCYP-R failed to generate specific amplification under the same conditions Figures 24 and 25. Both these primers were designed on mRNA sequences and failed to produce a positive amplification with the DNA extract of the target, *E. senticosus*. Consequently, these two primer sets were excluded from further optimization.

The primers set EleuFDS-F/EleuFDS-R, designed to amplify a 283 bp region, also demonstrated robust performance Figure 26. A well-defined band corresponding to the expected fragment size was consistently observed for *E. senticosus* (P124), confirming the efficiency of this primer set. However, all other *Eleutherococcus* species also produced positive amplification.

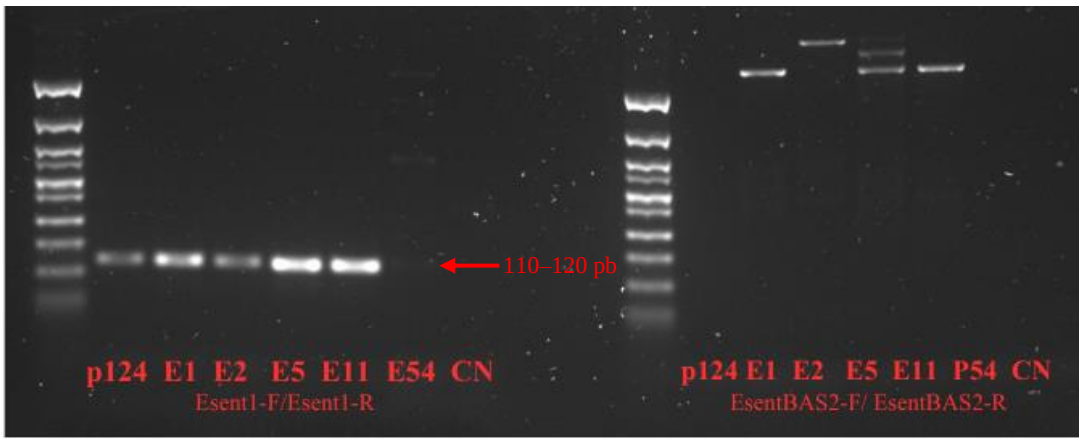

Figure 24 – PCR amplification using Esent1-F/Esent1-R and EsentBAS2-F/EsentBAS2-R at 60 °C

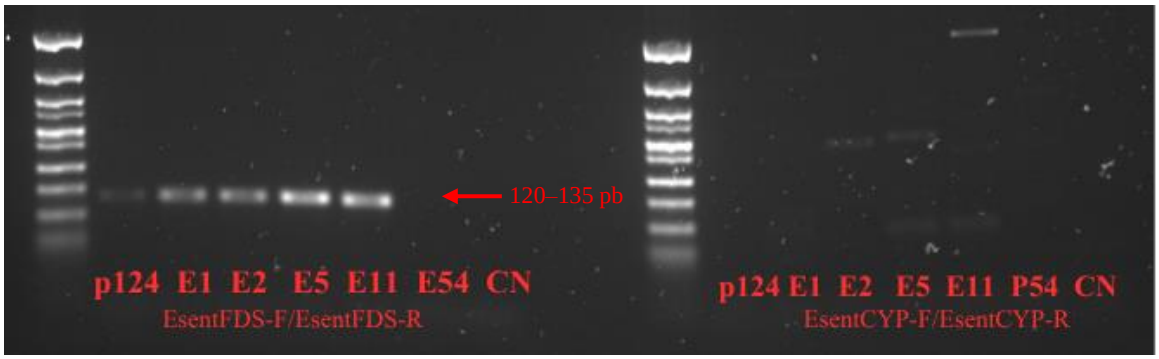

Figure 25 – PCR amplification using EsentFDS-F/EsentFDS-R and EsentCYP-F/EsentCYP-R at 60 °C

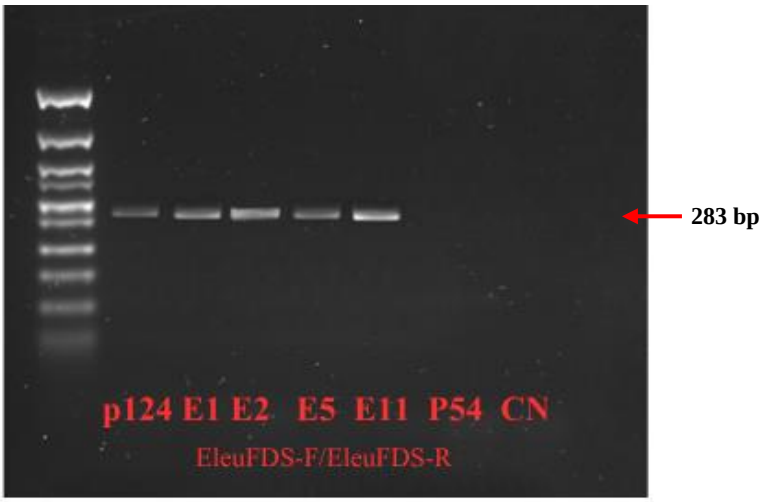

Figure 26 – PCR amplification using EleuFDS-F/EleuFDS-R at 60 °C

Cross-reactivity of species-specific

The primer sets EleuFDS-F/EleuFDS-R and Esent1-F/Esent1-R were further tested against several mixtures of DNA extracted from different medicinal plants used for similar therapeutic purposes as Siberian ginseng. In addition, cross-reactivity was also evaluated for the primer set EleuHRM-F/EleuHRM-R, which was designed to be genus-specific, aiming for species differentiation based on HRM analysis.

As shown in Figures 27 and 28, amplification occurred exclusively for the *E. senticosus* control, whereas none of the plant mixtures produced detectable amplicons. These results confirm that both EleuFDS and Esent1 maintain selectivity even in complex mixtures containing multiple non-target plant species.

In contrast, the EleuHRM-F/EleuHRM-R primer set displayed unintended amplification in some mixtures. As illustrated in Figure 35, the mixtures P6, P7 and P10 generated weak but visible amplicons despite not containing *E. senticosus*, indicating cross-reactivity with non-target species.

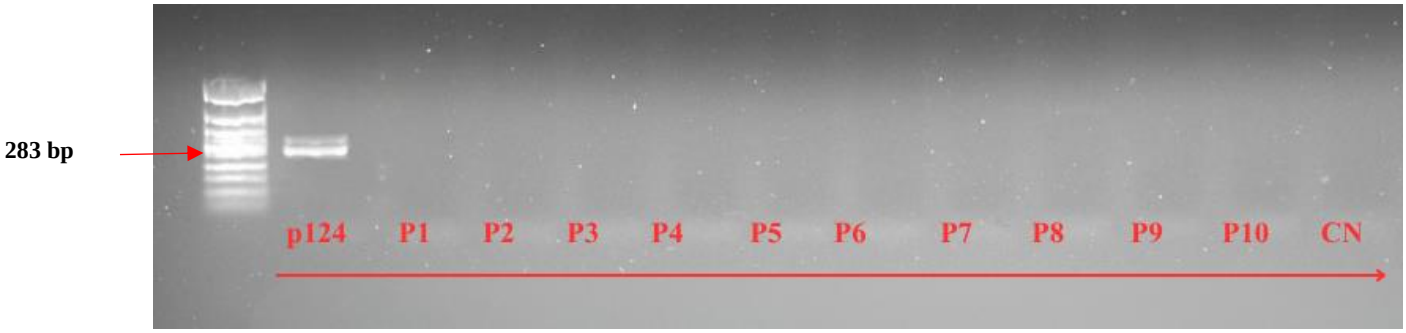

Figure 27- Cross-reactivity results for *E. senticosus* detection using EleuFDS-F/EleuFDS-R primers

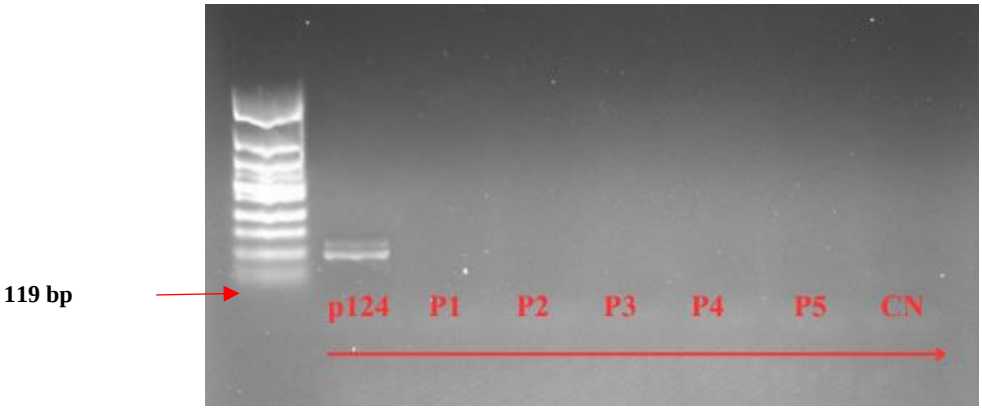

Figure 28- Cross-reactivity results for *E. senticosus* detection using Esent1-F/Esent1-R primer

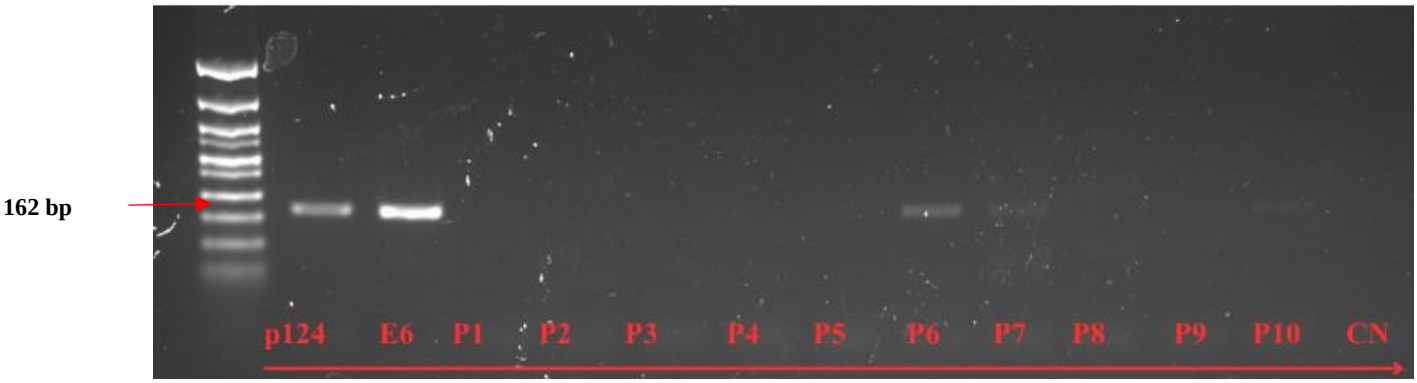

Figure 29- Cross-reactivity test for *E. senticosus* detection using EleuHRM-F/EleuHRM-R primers

4.2.3 Real-time PCR coupled with HRM analysis for *Eleutherococcus* species

The molecular discrimination of closely related species within the genus *Eleutherococcus* is challenging due to the high genetic similarity among its members. Therefore, with the aim of evaluating the discriminatory capacity of three primer pairs that were shown to be specific (Esent1, EleuFDS) or with high affinity (EleuHRM) for the *Eleutherococcus* genus, a real-time PCR using EvaGreen dye followed by HRM analysis was performed. The species tested included three positive controls of *E. senticosus* (P32, P59, P124) and samples of the other four *Eleutherococcus* species, namely *E. lasiogyne* (E3), *E. henryi* (E5), *E. leucorrhizus* (E9), and *E. divaricatus* (E11).

The assays were conducted with an annealing temperature of 65 °C and analyzed individually for each primer pair, allowing subsequent integration of the HRM results for discriminatory evaluation among species.

Real-time PCR and HRM using the Esent1-F/Esent1-R primer set

The Esent1-F/Esent1-R primer pair produced highly consistent amplification curves for all samples of *Eleutherococcus* sp.. The Cq values ranged from around 18 to 19 for *E. senticosus* and from 13 to 20 for the other *Eleutherococcus* species (Figure 36).

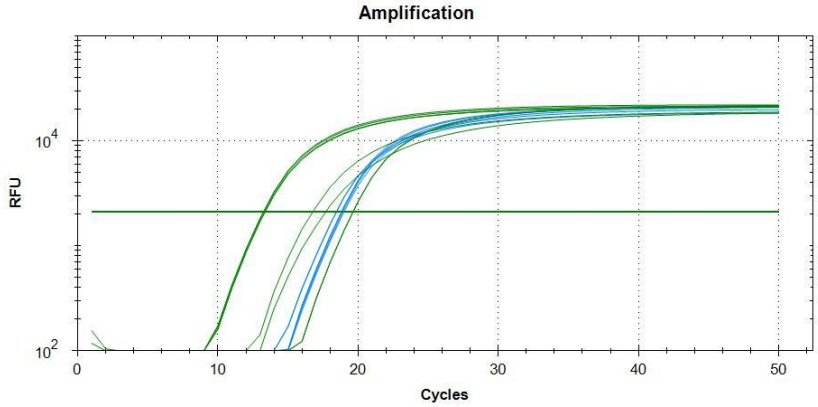

Figure 30 - Amplification curves obtained for the Esent1-F/R primer set by real-time PCR with EvaGreen dye (samples E3, E5, E9, E11 in green and P14, P59, P32 in blue).

The melting curve analysis revealed a single sharp melting peak for each sample, with values between 84–86 °C (Figure 37A), confirming that a single, specific amplicon was generated. Melt-peak analysis further supported the absence of non-specific products (Figure 37B).

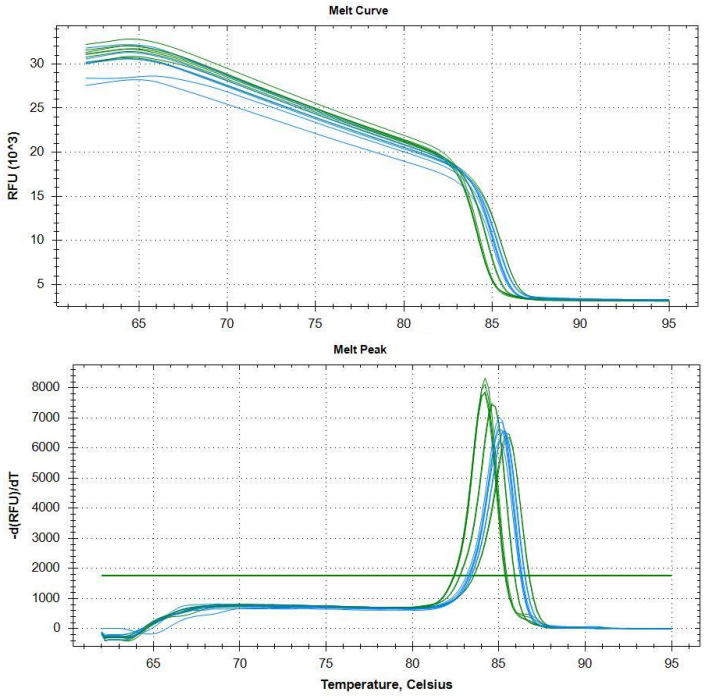

Figure 31 – Conventional melt curves (A) and melting peak (B) obtained by real-time PCR amplification with EvaGreen dye with Esent1-F/R primer set

Figure 38 shows the normalized HRM curves obtained, which demonstrate clear differences in curve shape among the species. The HRM software grouped the samples into five distinct clusters (Table 19). Notably, two of the *E. senticosus* controls (P59 and P124) grouped together (Cluster 2), whereas P32 consistently formed an independent cluster (Cluster 4).

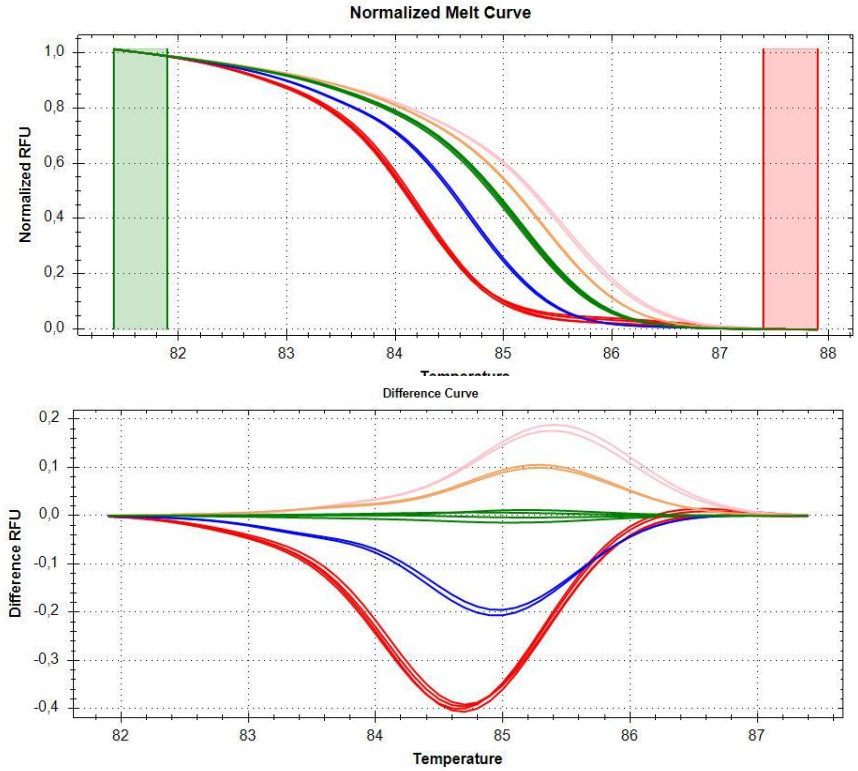

Figure 32 – Normalized melt and difference curves obtained by real-time PCR with EvaGreen dye using Esent1-F/R primer set (samples colors as described in Table 19).

Table 16- Cluster assignment and HRM confidence values for samples analyzed with primer set Esent1-F/ Esent1-R.

Sample Code	Species	Cluster Assignment	% Confidence	Ref
E9	*E. leucorrhizus*	Cluster 1	97.8	
E11	*E. divaricatus*	Cluster 1	95.4	
P59	*E. senticosus*	Cluster 2	99.8	
P124	*E. senticosus*	Cluster 2	99.8	
E3	*E. lasiogyne*	Cluster 3	99.5	
P32	*E. senticosus*	Cluster 4	99.8	
E5	*E. henryi*	Cluster 5	99.8	

The Esent1-F2/R2 primer showed strong interspecific discrimination, separating all non-target species from *E. senticosus*. However, intra-specific variation was detected among the *E.*

senticosus controls (P32 vs. P59 and P124), likely reflecting polymorphisms within the amplified region of the ITS locus. This could possibly the primers showed potential to be effective in distinguishing *E. senticosus* from other *Eleutherococcus* species.

Real-time PCR and HRM analysis using the EleuFDS-F/EleuFDS-R primer set

Amplification using EleuFDS-F/R primer set showed higher Cq values (ranging from 23 to28), indicating lower efficiency as compared to Esent1-F/R primer set. Consistent with the agarose gels (Figure 25), *E. senticosus* showed a latter amplification as compared to the other *Eleutherococcus* species evaluated (Figure 39, *E. senticosus* curves in blue).

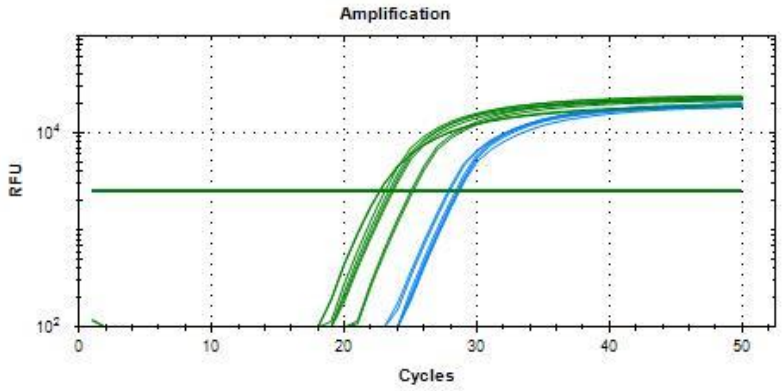

Figure 33 – Amplification curves obtained by real-time PCR with EvaGreen dye using the EleuFDS-F/EleuFDS-R primer set.

Conventional melting analysis showed a single amplicon for each sample, with melting peaks at ~79 °C detected across all samples with slight differences between the species (Figure 40). HRM analysis showed the existence of four clusters, with the three samples of *E. senticosus* being grouped together in Cluster 1 with a high percentage of confidence (>98.7%), E. *leucorrhizus* and *E. divaricatus* in Cluster 2, *E. lasiogyne* in Cluster 4 and *E. henryi* differentiated in Cluster 3, although with a lower confidence (86.8%) (Figure 41 and Table 20).

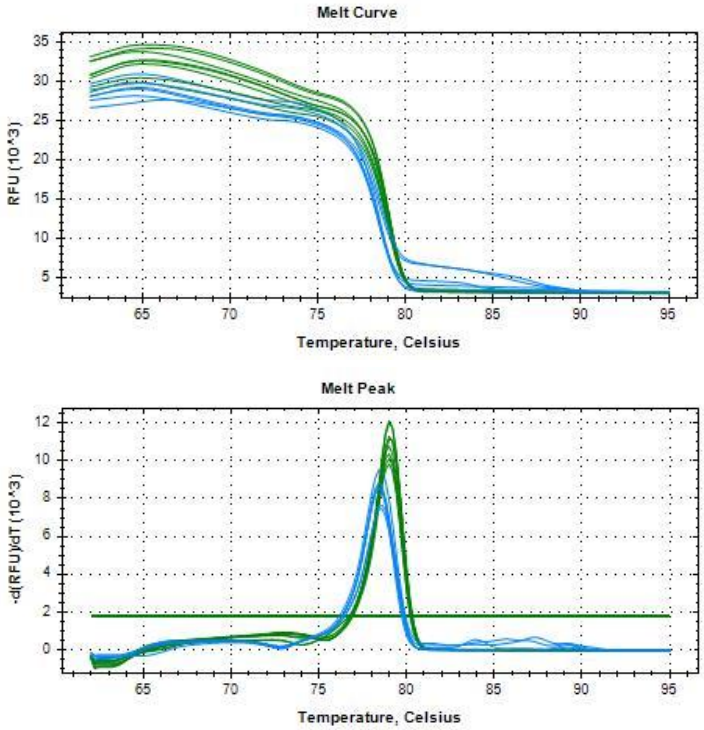

Figure 34 – Conventional melt curves (A) and melting peak (B) obtained by real-time PCR amplification with EvaGreen dye with EleuFDS-F/EleuFDS-R primer set

.

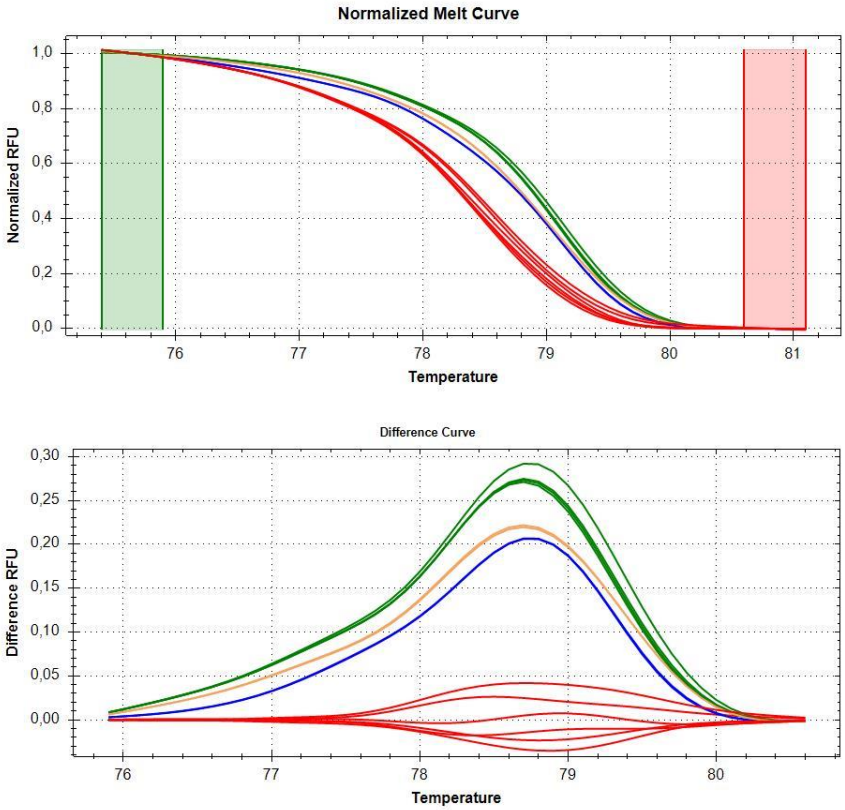

Figure 35 – Normalized melt and difference curves obtained by real-time PCR with EvaGreen dye using Esent1-F/R primer set (samples colors as described in Table 20).

Table 17 – HRM cluster assignment for samples analysed using the EleuFDS-F/EleuFDS-R primer set.

Sample Code	Species	Cluster Assignment	% Confidence	Ref
P32	*E. senticosus*	Cluster 1	98.7	
P59	*E. senticosus*	Cluster 1	99.7	
P124	*E. senticosus*	Cluster 1	98.8	
E3	*E. lasiogyne*	Cluster 4	91.2	
E5	*E. henryi*	Cluster 3	86.8	
E9	*E. leucorrhizus*	Cluster 2	100	
E11	*E. divaricatus*	Cluster 2	99.8	

The EleuFDS-F/R primer pair exhibited highly consistent amplification behaviour within *E. senticosus*, with all positive control samples clustering tightly and demonstrating intra-specific uniformity. In contrast, the non-target *Eleutherococcus* species formed clearly separated and non-overlapping clusters, indicating strong discriminatory capacity.

Given its stability, reliable amplification performance and robust ability to distinguish *E. senticosus* from closely related congeners, EleuFDS was selected as the optimal primer for subsequent validation across all *Eleutherococcus* accessions and commercial supplement samples.

Real-time PCR and HRM analyses using the EleuHRM-F/EleuHRM-R primer set

Figures 42, 43 and 44 show the results obtained using the primers initially designed for HRM analysis, namely EleuHRM-F/R. The amplification curves generally showed high Cq values, while the melting analysis revealed differences within the melting peak values, enabling the discrimination of the species in different clusters.

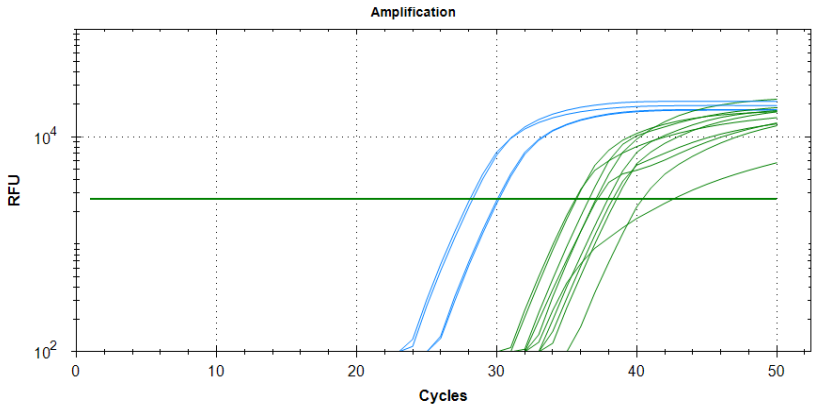

Figure 36 – Amplification curves obtained by real-time PCR with EvaGreen dye using the EleuHRM-F/EleuHRM-R primer set.

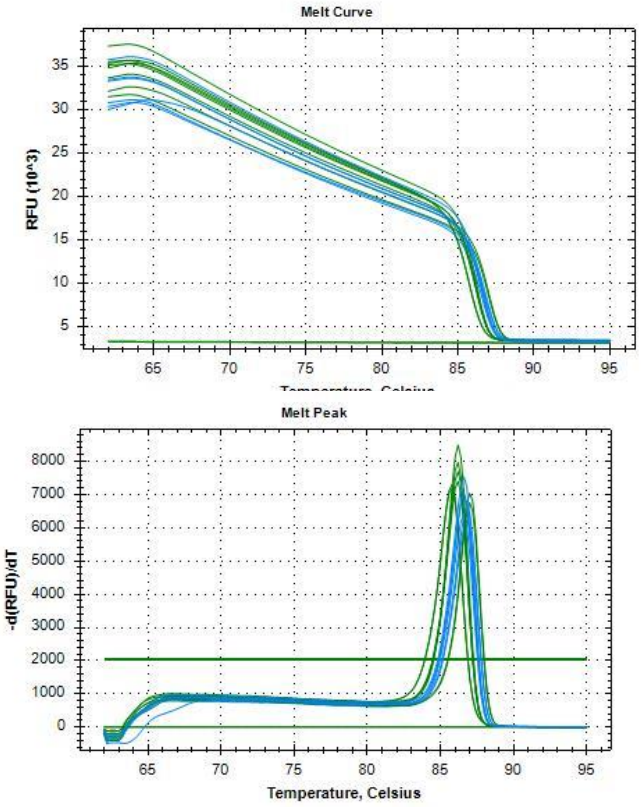

Figure 37 – Conventional melt curves (A) and melting peak (B) obtained by real-time PCR amplification with EvaGreen dye with EleuHRM-F/EleuHRM-R primer set

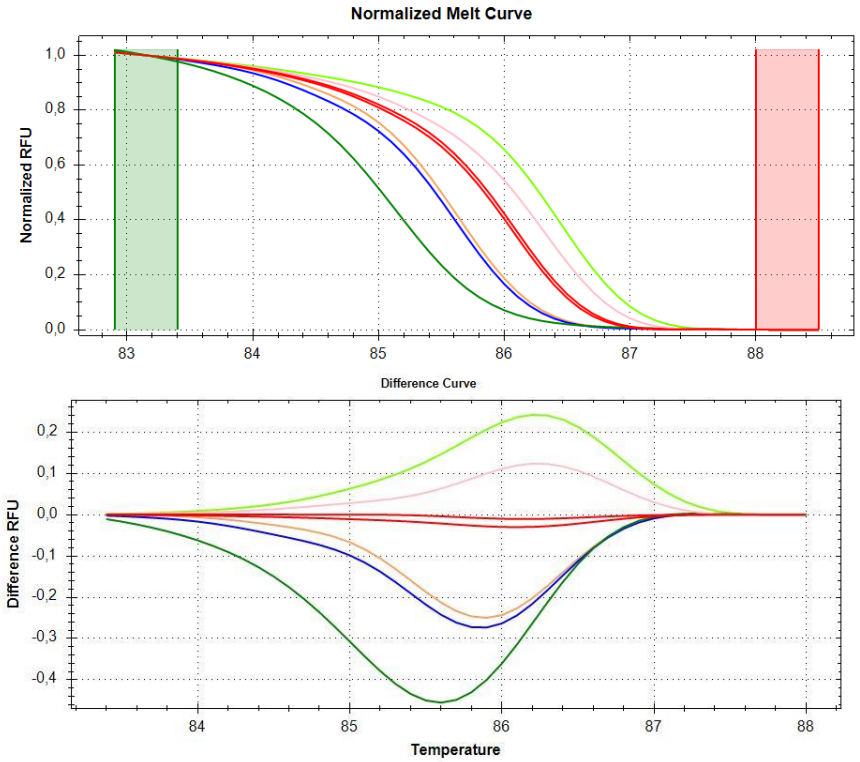

Figure 38 – Normalized melt and difference curves obtained by real-time PCR with EvaGreen dye using EleuHRM-F/EleuHRM-R primer set (sample colors as described in Table 21).

Table 18 – HRM cluster assignment for samples analyzed using the EleuHRM-F/EleuHRM-R primer

Sample Code	Species	Cluster Assignment	% Confidence	Ref
P32	*E. senticosus*	Cluster 1	99.7	
P124	*E. senticosus*	Cluster 1	99.8	
E3	*E. lasiogyne*	Cluster 2	100	
E5	*E. henryi*	Cluster 6	96.6	
E9	*E. leucorrhizus*	Cluster 3	93.8	
E11	*E. divaricatus*	Cluster 4	88.4	
P59	*E. senticosus*	Cluster 5	97.7	

Although the EleuHRM primer set was the only one capable of differentiating all the species, with *E. leucorrhizus* and *E. divaricatus* being placed in different clusters, again, one of the samples of *E. senticosus* was separated into a different cluster. Interestingly, with this primer set the sample exhibiting a different melting profile was P59, while with primers Esent1-F/Esent1-R it was P32.

Taken together, these findings indicate that, despite its high analytical sensitivity, EleuHRM does not provide the level of robustness required for reliable species authentication.

Selection of the optimal primer for species authentication

The combined real-time PCR and HRM results obtained for the three primer pairs evaluated (Esent1-F2/R2, EleuFDS-F/R, and EleuHRM-F/R) highlighted marked differences in amplification efficiency and discriminatory capacity. Although Esent1-F2/R2 demonstrated high amplification efficiency and produced clean single-peak melting profiles, its HRM clustering revealed intra-specific variation among the *E. senticosus* reference samples, with the accession P32 grouping independently from the remaining authentic controls. This behaviour reduces the reliability of Esent1 for downstream authentication, since intra-specific instability compromises the definition of a robust species-specific HRM signature. A similar output was observed with the EleuHRM-F/R primer set, which was able to discriminate all the evaluated species, however with one of the *E. senticosus* controls (P59) consistently forming a separate cluster. This lack of intra-specific coherence limits the applicability of both primer sets for high-confidence species discrimination.

In contrast, the EleuFDS-F/R primer exhibited lower amplification efficiency but generated highly stable melting profiles and demonstrated excellent discriminatory performance

of Siberian ginseng (*E. senticosus*). HRM clustering placed all *E. senticosus* authentic controls (P32, P59, P124) consistently within the same cluster, while all non-target *Eleutherococcus* species formed distinct and reproducible clusters. The absence of intra-specific variability among the controls, coupled with clear interspecific separation, indicates that EleuFDS-F/R provides the most robust and reliable HRM signature for *E. senticosus*. Therefore, based on the combined evaluation of amplification behaviour, HRM resolution, and species-level discrimination, EleuFDS-F/R was selected as the optimal primer pair for subsequent analyses, including testing against all available *Eleutherococcus* accessions and application to commercial supplement authentication.

4.2.4 Authentication of commercial products using the EleuFDS-F/R primer set

After selecting EleuFDS-F/R as the optimal primer pair for species authentication, the next step was to evaluate its performance on commercially available products declaring *E. senticosus* as ingredient. Only the samples listed in Tables 6 and 7 were analyzed in this stage, comprising encapsulated food supplements (S1–S4) and raw botanical materials or powders marketed as *E. senticosus* (Sg1–Sg7).

Before analyzing these commercial products, EleuFDS-F/R had previously been evaluated on an extended panel of authenticated *Eleutherococcus* species in order to define stable HRM clusters for interspecific comparison. These reference clusters (including *E. lasiogyne*, *E. henryi*, *E. leucorrhizus*, *E. divaricatus* and the authenticated *E. senticosus* material P124) served as a baseline for interpreting the HRM outputs of the commercial samples.

With the baseline clusters established, all commercial products were subjected to real-time PCR followed by HRM using EleuFDS-F/R under the same optimized conditions. The objective of this step was to determine whether the melting profiles obtained for each product matched the authenticated *E. senticosus* cluster, or instead corresponded to one of the clusters associated with non-target *Eleutherococcus* species. This approach allowed direct molecular authentication of labelled products and detection of potential substitution or adulteration.

All commercial products successfully amplified with EleuFDS-F/R, producing consistent amplification curves (Figure 51). Cq values were within the expected range for processed herbal matrices, demonstrating that the modified extraction protocol effectively removed PCR inhibitors. No signal was detected in the negative controls, confirming the absence of contamination. Overall, amplification behaviour across the commercial products was comparable to that of the authentic *E. senticosus* references.

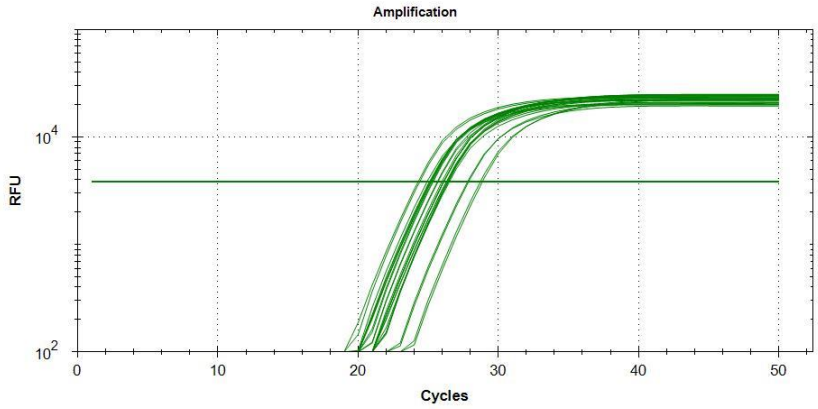

Figure 39 – Amplification curves obtained for the commercial Eleutherococcus samples using the EleuFDS-F/R primer set.

The melting curve analysis showed that all samples exhibited a single well-defined melting peak, with melt temperatures ranging from 79.2 to 79.8 °C (Figure 46). The melt peak profiles were sharp and homogeneous, indicating that EleuFDS-F/R amplified a single, specific product across all commercial samples, as previously observed for the reference material.

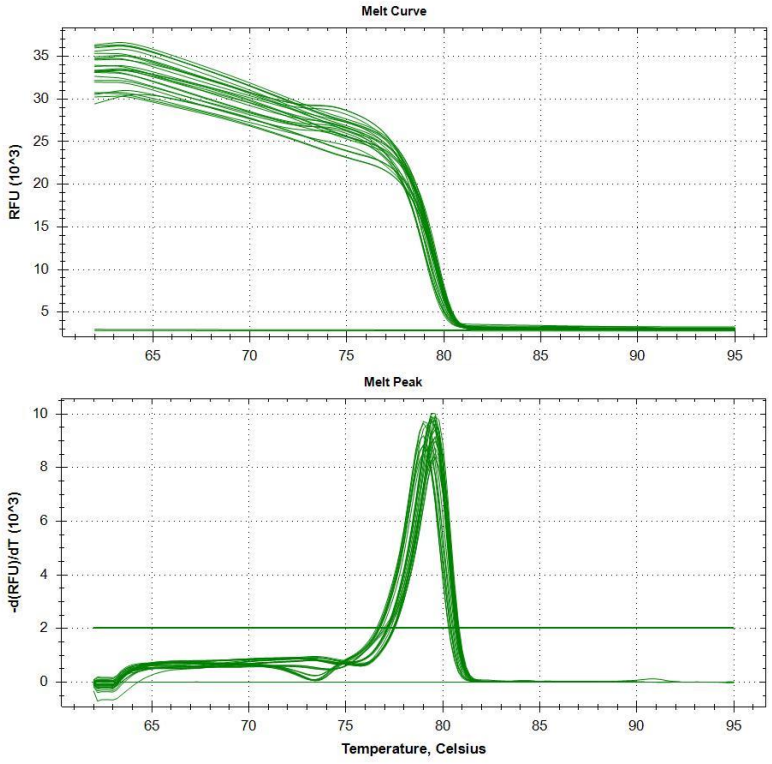

Figure 40 – Conventional melt curves (A) and melting peak (B) obtained by real-time PCR amplification with EvaGreen dye for the commercial Eleutherococcus samples using the EleuFDS-F/R primer set

Figure 42 and Table 23 show the HRM results obtained for the commercial samples, revealing distinct melting behaviors that become even more evident in the difference plot. The samples were divided into four well-defined clusters, with only samples Sg2 and Sg3 being grouped in the same cluster as *E. senticosus*. Despite being confirmed as belonging to the *Eleutherococcus* genus, all the other samples were not authenticated as Siberian ginseng, as the labeling was not confirmed. They may consist of other species of the same genus or mixtures of those with *E. senticosus*. Further studies would be necessary for the identification of these samples.

Overall, these results confirm that EleuFDS-F/R provides a reliable and discriminating molecular tool for the authentication of consumer-ready herbal products declared as being Siberian ginseng (*E. senticosus*).

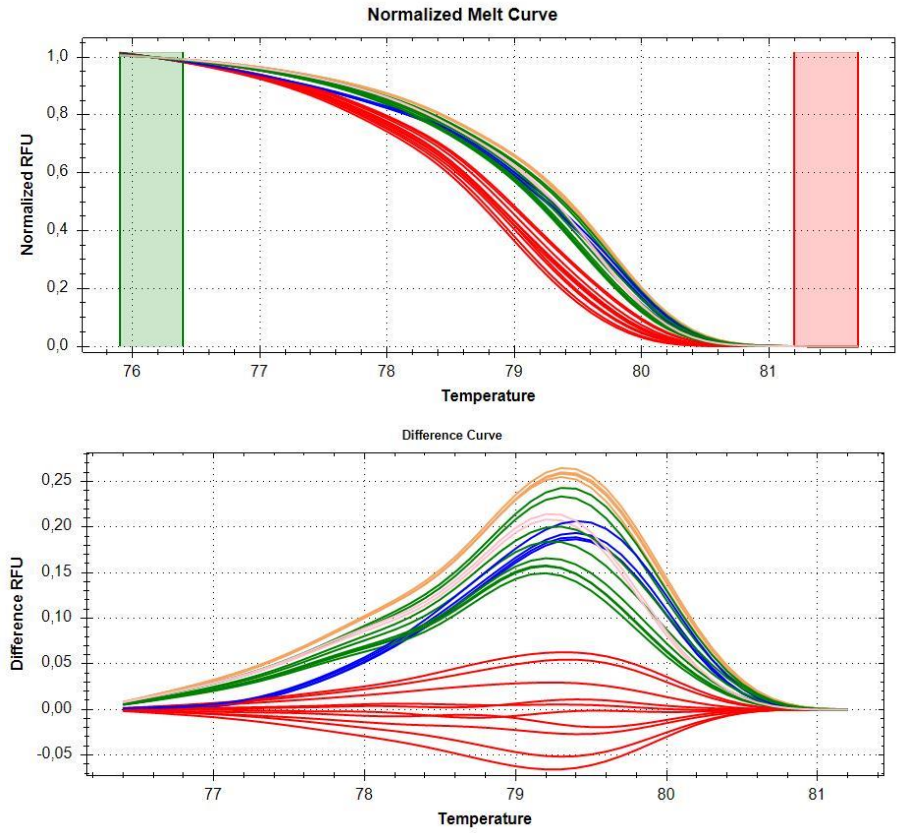

Figure 41 – Normalized melt and difference curves obtained by real-time PCR with EvaGreen dye using EleuFDS-F/R primer set (sample colors as described in Table 23).

Table 19 – HRM cluster assignment for commercial samples analyzed using EleuFDS-F/R primer set

Code	Sample	Cluster Assignment	% Confidence	Ref
P124	*E. senticosus*	Cluster 1	98.7	
SG2	*Herbal product*	Cluster 1	98.2	
SG3	*Herbal product*	Cluster 1	97.0	
P59	*E. senticosus*	Cluster 1	99.4	
P32	*E. senticosus*	Cluster 1	98.8	
SG1	*Herbal product*	Cluster 2	97.2	
SG4	*Herbal product*	Cluster 2	97.7	
SG5	*Herbal product*	Cluster 2	97.0	
S2	*Food supplement*	Cluster 2	97.6	
S3	*Food supplement*	Cluster 3	98.4	
S4	*Food supplement*	Cluster 3	98.6	
S1	*Food supplement*	Cluster 4	94.3	
SG7	*Herbal product*	Cluster 4	96.7	
SG6	*Herbal product*	Cluster 5	94.3	

5. Conclusions

The consumption of medicinal plant-based products and botanical supplements has been steadily increasing, while reports of mislabeling, substitution, and adulteration of raw materials continue to accumulate. In this context, DNA-based identification methods particularly those supported by real-time PCR and HRM are emerging as promising tools to complement or replace traditional morphological and chemical approaches, which are often insufficient for processed matrices, complex mixtures, or dried and powdered materials.

In this study, the applicability of conventional PCR, real-time PCR, and HRM techniques for authenticating two commercially important plants, *Rhodiola rosea* and *Eleutherococcus senticosus*, was evaluated. For both species, two approaches were followed, namely the attempt of designing primers that would be specific for the targeted species and the design of primers that would allow differentiating the target species from others of the same genus based on HRM analysis.

In the case of *Rhodiola*, the results consistently highlighted the limitations of the evaluated primers. Although some systems displayed good amplification efficiency and the ability to detect sequence variation, none of them produced a stable and exclusive HRM pattern for *R. rosea*. The RD-HRM2, RodR3/RodR2, and RodR2/RodR2 primers all showed intraspecific variability, with *R. rosea* samples distributed across several distinct clusters, while non-target species (*R. kirilowii*, *R. heterodonta*, *R. crenulata*, *R. stephanii*, among others) grouped together with the target species in more than one of these clusters. Thus, although the assays demonstrated the high sensitivity of HRM for detecting polymorphisms within the *Rhodiola* genus, the lack of a unique and reproducible melting profile renders these primers unsuitable, under the tested conditions, as diagnostic markers for unequivocal authentication of *R. rosea* in commercial matrices.

In contrast, the results obtained for *Eleutherococcus senticosus* were clearly more encouraging. Among the three systems tested, the EleuFDS-F/R primer pair stood out by combining good amplification efficiency with high robustness in HRM: all *E. senticosus* positive controls consistently clustered together, while congeneric species (*E. lasiogyne*, *E. henryi*, *E. leucorrhizus*, and *E. divaricatus*) formed separate and well-defined clusters. The absence of relevant intraspecific variability in *E. senticosus*, combined with clear separation from non-target species, enabled the establishment of a reliable melting profile signature for the species.

Applying the EleuFDS-F/R primer to commercial food supplements and herbal products labeled as containing *E. senticosus* further demonstrated the practical feasibility of the method.

All products analyzed amplified efficiently, and the HRM profiles obtained were consistent with the previously defined clusters for the target species, however only two samples were authenticated as Siberian ginseng (*E. senticosus*). The other samples formed different clusters, which suggests they may be either from other *Eleutherococcus* species or mixtures of *E. senticosus* with other plants.

Taken together, these results allow us to conclude that, for *Rhodiola rosea*, the evaluated primers did not achieve the specificity and consistency required for routine authentication, indicating the need to design new markers, possibly at other loci and supported by prior sequencing of a larger number of botanically authenticated accessions. Conversely, for *Eleutherococcus senticosus*, the system based on the EleuFDS-F/R primer combined with HRM analysis proved suitable for species-level identification and successfully confirmed the authenticity of only two of the analyzed supplements, suggesting a high level of adulteration in these products.

REFERENCES

Amidžić M, Banović Fuentes J, Banović J, Torović L. Notifications and Health Consequences of Unauthorized Pharmaceuticals in Food Supplements. Pharm Basel Switz. 2023;11(5):154.

Bernatoniene J, Jakstas V, Kopustinskiene DM. Phenolic Compounds of Rhodiola rosea L. as the Potential Alternative Therapy in the Treatment of Chronic Diseases. Int J Mol Sci. 2023;24(15):12293.

Bezerra RJ, Calheiros AS, da Silva Ferreira NC, da Silva Frutuoso V, Alves LA. Natural Products as a Source for New Anti-Inflammatory and Analgesic Compounds through the Inhibition of Purinergic P2X Receptors. Pharmaceuticals (Basel). 2013;6(5):650-8.

Booker A, Jalil B, Frommenwiler D, Reich E, Zhai L, Kulic Z, Heinrich M. The authenticity and quality of Rhodiola rosea products. Phytomedicine. 2016 Jun;23(7):754-62.

Brekhman II, Dardymov IV. New substances of plant origin which increase nonspecific resistance. Annual Review of Pharmacology. 1969;9:419–430.

Calapai G. European legislation on herbal medicines: a look into the future. Drug Saf. 2008;31(5):428-31.

Chang Y, Jiang Y, Chen J, Li S, Wang Y, Chai L, Ma J, Wang Z. Comprehensive analysis of Eleutherococcus senticosus fruits based on UPLC-MS/MS and GC-MS: A rapid qualitative analysis. Food Science & Nutrition. 2023;12(3):1911–1927.

Chen S, Yao H, Han J, Liu C, Song J, Shi L, et al. Validation of the ITS2 region as a novel DNA barcode for identifying medicinal plant species. PLoS One. 2010;5(1):8613.

Cheng T, Xu C, Lei L, Li C, Zhang Y, Zhou S. Barcoding the kingdom Plantae: new PCR primers for ITS regions of plants with improved universality and specificity. Mol Ecol Resour. 2016;16(1):138-49.

Cheng X, Su X, Chen. Biological ingredient analysis of traditional Chinese medicine preparation based on high-throughput sequencing: the story for Liuwei Dihuang Wan. Sci Rep. 2014;(4):5147.

Chiang HM, Chen HC, Wu CS, Wu PY, Wen KC. Rhodiola plants: Chemistry and biological activity. J Food Drug Anal. 2015;23(3):359-369.

Coghlan ML, Haile J, Houston J, Murray DC, White NE, Moolhuijzen P, et al. Deep Sequencing of Plant and Animal DNA Contained within Traditional Chinese Medicines Reveals Legality Issues and Health Safety Concerns. PLoS Genet. 2012;8(4):e1002657.

Costa J, Amaral JS, Fernandes TJR, Batista A, Oliveira MBPP, Mafra I. DNA extraction

from plant food supplements: Influence of different pharmaceutical excipients. Mol Cell Probes. 2015;29(6):473-478.

Costa J, Campos B, Amaral J, Nunes ME, Oliveira MBPP, Mafra I. HRM analysis targeting ITS1 and matK loci as potential DNA mini-barcodes for the authentication of Hypericum perforatum and Hypericum androsaemum in herbal infusions. Food Control. 2016;61:105-114.

Cropley M, Banks AP, Boyle J. The Effects of Rhodiola rosea L. Extract on Anxiety, Stress, Cognition and Other Mood Symptoms. Phytother Res. 2015;29(12):1934-9.

Davydov M, Krikorian AD. Eleutherococcus senticosus (Rupr. & Maxim.) Maxim. (Araliaceae) as an adaptogen: A closer look. Journal of Ethnopharmacology. 2000;72(3):345–393.

Doganay-Knapp K, Orland A, König GM, Knöss W. The potential of three different PCR-related approaches for the authentication of mixtures of herbal substances and finished herbal medicinal products. Phytomedicine. 2018;43:60-67.

Doyle JJ, Doyle JL. A rapid DNA isolation procedure for small quantities of fresh leaf tissue. Phytochemical Bulletin. 1990;19:11–15.

El-Ahmady SH, Ashour ML. Advances in testing for adulteration of food supplements. In: Downey G, ed. Advances in food authenticity testing. Cambridge: Woodhead Publishing; 2016. p. 667-699.

EU. Directive 2002/46/EC of the European Parliament and of the Council of 10 June 2002. Official Journal of the European Communities. 2002;45:51–57.

European Medicines Agency (EMA). Herbal medicinal products. 2024.

Fang G, et al. Influence of polyphenols on plant DNA extraction and PCR amplification. Plant Methods. 2019;15:1–8.

Franz C, Chizzola R, Novak J, Sponza S. Botanical species being used for manufacturing plant food supplements (PFS) and related products in the EU. Food Funct. 2011;2(12):720–730.

Frigerio J, Agostinetto G, Mezzasalma V, De Mattia F, Labra M, Bruno A. DNA-based herbal teas' authentication. Plants. 2021;10(10):2120.

Ganzera M, Yayla Y, Khan IA. Analysis of marker compounds of Rhodiola rosea. Chem Pharm Bull. 2001;49(4):465-7.

Garcia-Alvarez A, et al. Usage of plant food supplements across six European countries. PLoS One. 2014;9(3):92265

Graczyk F, et al. Phenolic profile and activity of Eleutherococcus fruits and roots. Molecules. 2022;27(17):5579.

Grazina L, Amaral JS, Mafra I. Botanical origin authentication of dietary supplements by DNA-based approaches. Compr Rev Food Sci Food Saf. 2020;19(3):1080-1109

Grazina L, Mafra I, Monaci L, Amaral JS. Mass spectrometry-based approaches to assess botanical authenticity. Compr Rev Food Sci Food Saf. 2023;22(5):3870–3909.

Haynes E, Jimenez E, Pardo MA, Helyar SJ. The future of NGS in food authenticity testing. Food Control. 2019;101:134-143.

Hebert PD, Cywinska A, Ball SL, deWaard JR. Biological identifications through DNA barcodes. Proc Biol Sci. 2003;270:313-21.

Herrmann MG, et al. Amplicon DNA melting analysis comparison. Clin Chem. 2006;52(3):494-503.

Heubl G. DNA-based authentication of Chinese medicinal plants. Planta Med. 2010;76(17):163-74.

Hollingsworth PM, et al. A DNA barcode for land plants. PNAS. 2009;106(31):12794-7

Hwang S, Kim JH, Moon JC, Jang CS. Chloroplast markers for detecting rice-derived ingredients. Genes Genomics. 2015;37(12):1027–1034.

Ivanova NV, et al. Authentication of herbal supplements using NGS. PLoS One. 2016;11(5):0156426.

Jobes DV, Hurley DL, Thien LB. Plant DNA isolation removing polyphenolics. Taxon. 1995;44(3):379–386.

Kennedy DO, Scholey AB, Wesnes KA. Ginseng cognitive effects. Nutr Neurosci. 2001;4(4):295–310.

Kim N, Kwon JS, Kang WH, Yeom SI. High-Resolution Melting Genotyping. Methods Mol Biol. 2023;2638:337-349.

Kircher M, Kelso J. High-throughput DNA sequencing concepts. Bioessays. 2010;32:524–536.

Kress WJ, Erickson DL. A two-locus global DNA barcode for plants. PLoS One. 2007;2(6):e508.

Li X, Yang Y, Henry RJ, Rossetto M, Wang Y, Chen S. Plant DNA barcoding: from gene to genome. Biol Rev. 2015;90(1):157-66.

Little DP, Jeanson ML. DNA barcode authentication of saw palmetto. Sci Rep. 2013;3:3518.

Liu Z, Yang MQ, Zuo Y, Wang Y, Zhang J. Fraud detection of herbal medicines. Crit Rev Anal Chem. 2022;52(7):1606-1623.

Ma D, et al. Differentiation of Rhodiola species via UHPLC fingerprints. Molecules.

2021;26(22):6855.

Marchev AS, Koycheva IK, Aneva IY, Georgiev MI. Evaluation of Rhodiola species by NMR an HPLC. Phytochem Anal. 2020;31(6):756-769.

Marques AEF, Oliveira PMF, Macedo I. Estudo da atividade farmacológica da Rhodiola rosea. J Biol Pharm Agric Manag. 2023;15:295-305.

Malík M, Tlustoš P. Nootropic herbs as cognitive enhancers. Plants. 2023;12(6):1364.

Maruyama T, et al. Authentication of Eleutherococcus senticosus by DNA. Planta Med. 2008;74(7):787–789.

Michel CI, Meyer RS, Taveras Y, Molina J. ITS2 as plant DNA barcode in herbal medicines. J Appl Res Med Aromat Plants. 2016;3(3):94-100.

Mishra P, et al. DNA barcoding to overcome herbal authentication challenges. Plant Biotechnol J. 2016;14(1):8-21.

Moraes DF, Coutinho, Still DW, Lum MR, Hirsch AM. DNA-based authentication of botanicals. Planta Med. 2015 Jun;81(9):687-95.

Navarro E, Serrano-Heras G, Castaño MJ, Solera J. Real-time PCR detection chemistry. Clin Chim Acta. 2015;439:231-50.

Nicotra G. Rhodiola rosea – a useful adaptogen. Nutrafoods. 2010;9:29–33.

Panossian A, Wikman G, Sarris J. Rosenroot: traditional use, chemistry, pharmacology. Phytomedicine. 2010;17(7):481-93.

Paran I, Michelmore RW. PCR-based markers for downy mildew resistance. Theor Appl Genet. 1993;85(8):985-93.

Parveen I, Gafner S, Techen N, Murch SJ, Khan IA. DNA barcoding for botanicals. Planta Med. 2016;82(14):1225-35.

Porebski S, Bailey LG, Baum BR. Modified CTAB extraction for polysaccharide-rich plants. Plant Mol Biol Rep. 1997;15(1):8–15.

Pu Wei, Zhang MY, Bai RY, et al. Anti-inflammatory effects of Rhodiola. Biomed Pharmacother. 2020;121:109552.

Purushothaman N, et al. Tiered barcode tool for Cassia. Genet Mol Res. 2014;13(2):122.

Quail MA, et al. Comparison of NGS platforms. BMC Genomics. 2012;13:341.

Raclariu AC, Heinrich M, Ichim MC, de Boer H. Benefits and limitations of barcoding/metabarcoding. Phytochem Anal. 2018;29:123-128.

Rocha T, Amaral JS, Oliveira MBPP. Adulteration of dietary supplements. Compr Rev Food Sci Food Saf. 2016;15:43–62.

Ruhsam M, Hollingsworth PM. Authentication of Eleutherococcus and Rhodiola

supplements. Pharm Biomed Anal. 2018;149:403-409.

Sasikumar B, Swetha VP, Parvathy VA, Sheeja TE. Authenticity testing of herbs. In: Advances in food authenticity testing. 2016;585–624.

Schrader C, et al. PCR inhibitors. J Appl Microbiol. 2012;113:1014–1026

Selvaraj D, et al. DNA barcoding for plant biodiversity conservation. Plant Breed Biotechnol. 2013;1:320–32.

Sen T, Samanta SK. Medicinal plants, health and biodiversity. Adv Biochem Eng Biotechnol. 2015;147:59-110

Sgamma T, et al. DNA barcoding for industrial QA. Planta Med. 2017;83(14-15):1117-1129

Shah AP, et al. Adulteration in Brahmi herbal products. bioRxiv. 2022.

Shokralla S, Spall JL, Gibson JF, Hajibabaei M. NGS for environmental DNA. Mol Ecol. 2012;21(8):1794–1805.

Smillie TJ, Khan IA. Identifying and authenticating botanical products. Clin Pharmacol Ther. 2010;87(2):175-86.

Soares S, Amaral JS, Oliveira MBPP, Mafra I. Improving DNA isolation from honey. Food Control. 2015;48:130–136.

Staats M, et al. Advances in DNA metabarcoding. Anal Bioanal Chem. 2016;408:4615–4630.

Sucher NJ, Hennell JR, Carles MC. DNA fingerprinting and NGS in plants. Methods Mol Biol. 2012;862:13–22.

Sun Wei, Li JJ, Xiong C, Zhao B, Chen SL. Power of Bar-HRM technology. Front Plant Sci. 2016;7:367.

Techen N, Parveen I, Pan Z, Khan IA. DNA barcoding of medicinal plant material. Curr Opin Biotechnol. 2014;25:103-10.

Untergasser A, Cutcutache I, Koressaar T, Ye J, Faircloth BC, Remm M, Rozen SG. Primer3—new capabilities. Nucleic Acids Res. 2012;40:e115.

Varma A, et al. Plant polysaccharides impact on DNA isolation. Plant Mol Biol Rep. 2007;25:53–64.

Vossen RH, Aten E, Roos A, den Dunnen JT. HRM analysis. Hum Mutat. 2009;30(6):860-6.

Wang X, Zhang A, Yan G, Han Y, Sun H. UHPLC-MS for TCM characterization. Trends Anal Chem. 2014;63:180–7.

WHO. Traditional medicine strategy 2014–2023. Geneva: WHO; 2013.

Wilkins T, Smart L. DNA isolation from polyphenolic tissues. Plant Mol Biol Rep. 1996;14:11–17.

Wittwer CT, Reed GH, Gundry CN, Vandersteen JG, Pryor RJ. HRM genotyping using LCGreen. Clin Chem. 2003;49(6):853-60.

Xin T, Li X, Yao H, Lin Y, Ma X, Cheng R, et al. Survey of commercial Rhodiola products. Sci Rep. 2015;5:8337.

Xue CY, Xue HG. Authentication of Drynaria fortunei via Scorpion PCR. Planta Med. 2008;74(11):1416-20.

Yao H, Song J, Liu C, Luo K, Han J, Li Y, et al. ITS2 as universal DNA barcode. PLoS One. 2010;5(10):13102.

Yao Lu, Deng B, Xu L, Liu H, Song Y, Lin F. Effects of Rhodiola supplementation on exercise. Front Nutr. 2022;9:856287.

Zhu H, Zhang H, Xu Y, Laššáková S, Korabečná M, Neužil P. PCR past, present and future. Biotechniques. 2020;69(4):317-325.

Zhu Liu, Liu Z, Ren Y, Wu X, Liu Y, Wang T, et al. Neuroprotective effects of salidroside. Phytother Res. 2021;35(10):5767-5780.

Appendix

Table S1 – List of plants used to prepare the mixtures in the cross-reactivity tests *Eleutheroccocus*.

	ID	ID plant
P1	M01	*Hipericão do Gerês*
	M02	*Condurango*
	M03	*Passiflora*
	M04	*Erva cidreira*
	M05	*Artemísia*
P2	M06	*Jasmim*
	M07	*Camomila*
	M08	*Cipreste*
	M09	*Erva serpente*
	M10	*Aroeira*
P3	M11	*Cipó mil homens*
	M12	*Eleuterococus I ginseng siberiano*
	M13	*Agripalma*
	M14	*Congossa / Pervinca*
	M15	*Nêveda / Calaminta*
P4	M16	*Alecrim*
	M17	*Erva Moura*
	M18	*Cidreira*
	M19	*Funcho*
	M20	*Espinheiro Alvar*
P5	M21	*Gerivão / Verbena*
	M22	*Ginkgo Biloba*
	M23	*Cavalinha*
	M24	*Hipericão Kneip*
	M25	*Bistorta*
	M26	*Valeriana*
P6	M27	*Angelica*
	M28	*Ginseng Branco*
	M29	*Guaraná*
	M30	*Noz de Kola*
	M31	*Ginkgo Biloba*
	M32	*Ginseng Siberiano*
P7	M33	*Erva Mate*
	M34	*Rooibos Relax Anti-Stress*
	M35	*Tisana Ginseng e Vitalidade*
	M36	*Hipericão Premium*
	M37	*Passiflora Premium*
	M38	*Moringa Oleifera*

P8	M39	*Marapuama*
	M40	*Tisana Bom Sono*
	M41	*Mulungu*
	M42	*Insulina Vegetal*
	M43	*Laranja amarga*
P9	M44	*Tilia*
	M45	*Centella asiatica*
	M46	*Erva-Principe*
	M47	*Tisana Calmante*
	M48	*Limoeiro*
P10	M49	*Nervcalmflora*
	M50	*Bom Sono*
	M51	*Neveda*
	M52	*Sophora japonica*

Table 11 – List of plants used to prepare the mixtures in the cross-reactivity tests *Rhodiola*

	ID	**ID plant**
ML1	N01	*Hypericum androsaemum*
	N02	*Marsdenia condurango*
	N03	*Passiflora incarnata*
	N04	*Melissa officinalis*
ML2	N05	*Artemisia vulgaris*
	N06	*Jasminum grandiflorum*
	N07	*Matricaria chamomilla*
	N08	*Cupressus sempervirens*
ML3	N09	*Mikania hirsutissima*
	N10	*Lavandula stoechas*
	N11	*Aristolochia esperanzae kuntze*
	N12	*Eleutherococcus senticosus*
ML4	N13	*Cymbopogon citratus*
	N14	*Vinca minor*
	N15	*Tilia europaea*
	N16	*Rosmarinus officinalis*
ML5	N17	*Solanum nigrum*
	N18	*Melissa officinalis*
	N19	*Foeniculum vulgare*
	N20	*Crataegus oxyacantha*
ML6	N21	*Verbena officinalis*
	N22	*Ginkgo biloba*
	N23	*Equisetum arvense*
ML7	N24	*Hypericum perforatum*
	N25	*Persicaria bistorta*
	N26	*Valeriana officinalis*
	N27	*Angelica archangelica*

ML8	N28	*Panax ginseng*
	N29	*Paullinia cupana*
	N30	*Cola nitida*
	N31	*Ginkgo biloba*
	N32	*Eleutherococcus senticosus*
	N33	*Ilex paraguariensis*
ML9	N34	*Ginkgo biloba*
	N35	*Valeriana officinalis*
	N36	*Hypericum perforatum*
	N37	*Passiflora incarnata*
	N38	*Moringa oleifera*
ML10	N39	*Ptychopetalum olacoides*
	N40	*passiflora*
	N41	*Erythrina*
	N42	*Myrcia citrifólia*
	N43	*Citrus aurantium*